

Supplementary Information

In Silico Design Criteria for High Blocking Barrier Uranium(III) SIMs

Sourav Dey and Gopalan Rajaraman*

Department of Chemistry, Indian Institute of Technology Bombay, Powai, Mumbai-400076

Email: rajaraman@chem.iitb.ac.in

Computational Details

The U(III)-OH₂ and U(III)-OH bond length in all the in silico models was kept fixed at 2.52 and 2.11 Å, respectively, from the earlier studies.¹⁻⁴ Partial optimisation of hydrogen in the seventeen best performing in silico models (see Figure S1) was performed with UB3LYP functional using Gaussian 09 suite of programme.⁵⁶ We have used CRENBL ECP basis set⁷ for Uranium and 6-31G** basis set⁸ for rest of the atoms. The quadratic convergence method was followed to obtain the most stable structure. The shape measurement of all the in silico models has been carried out in SHAPE v2.1.⁹

All the post-Hartree Fock *ab initio* calculations were performed by the MOLCAS 8.0 programme package.¹⁰ We have used Douglas-Kroll-Hess (DKH) Hamiltonian to take into account the scalar relativistic effect in the calculation.^{11, 12} The Cholesky decomposition technique to reduce the disk space.¹¹ All the basis sets were taken from the ANO-RCC library implemented in MOLCAS 8.0 package.¹⁰ We have used the following contraction scheme: [U.ANO-RCC...9s8p6d4f2g1h.], [O.ANO-RCC...4s3p2d1f.], and [H.ANO-RCC...2s.] in the basis set of U, O and H respectively in all the in silico models. The spin-free wave functions for CASSCF (complete active space self-consistent field) calculation were generated with 3 electrons in seven 5f orbitals, i.e., with CAS (3,7) active space. We have computed the energy of 35 quartets and 112 doublets within this active space. Thereafter single state CASPT2 (using “NOMULT” keyword) calculations were performed to include the dynamic correlation in the next step (for the best performing in silico models, see Figure S1). In CASPT2 calculations, the roots of the doublet spin state for some models were reduced to achieve the converge. The IPEA value of 0.25 was used for the CASPT2 calculation. The spin-orbit interaction between all the spin-free states has been taken into account by the RASSI-SO methodology. The magnetic susceptibility, g tensors, barrier height and QTM were computed by the SINGLE_ANISO module of MOLCAS, which interfaces with the energies of all spin-orbit states computed from the RASSI-SO step. The crystal field parameters and m_J composition of the ground state has been extracted with isoelectronic lanthanide analogue Nd(III) as SINGLE_ANISO module of MOLCAS 8.0 programme package does not support calculations of the same with actinides.¹³ In a nutshell, the magnetic property was computed by a full *ab initio* approaching where spin-orbit coupling was taken into account perturbatively.

The magnetic anisotropy of the X-ray structure and optimised geometries of U(III) complexes (**1-23**, **8F** and **15F**) were estimated by *ab initio* CAS(3,7)SCF/RASSI-SO/SINGLE_ANISO calculations. It is noteworthy to mention that CASPT2 calculations were not performed on these complexes due to computational limitations. We have used the VTZP quality basis set for U, VDZP quality basis set for the atoms in the first coordination sphere and VDZ quality basis set for the atoms in the secondary coordination sphere for the CASSCF calculations. The other computational details are the same as described before for model complexes.

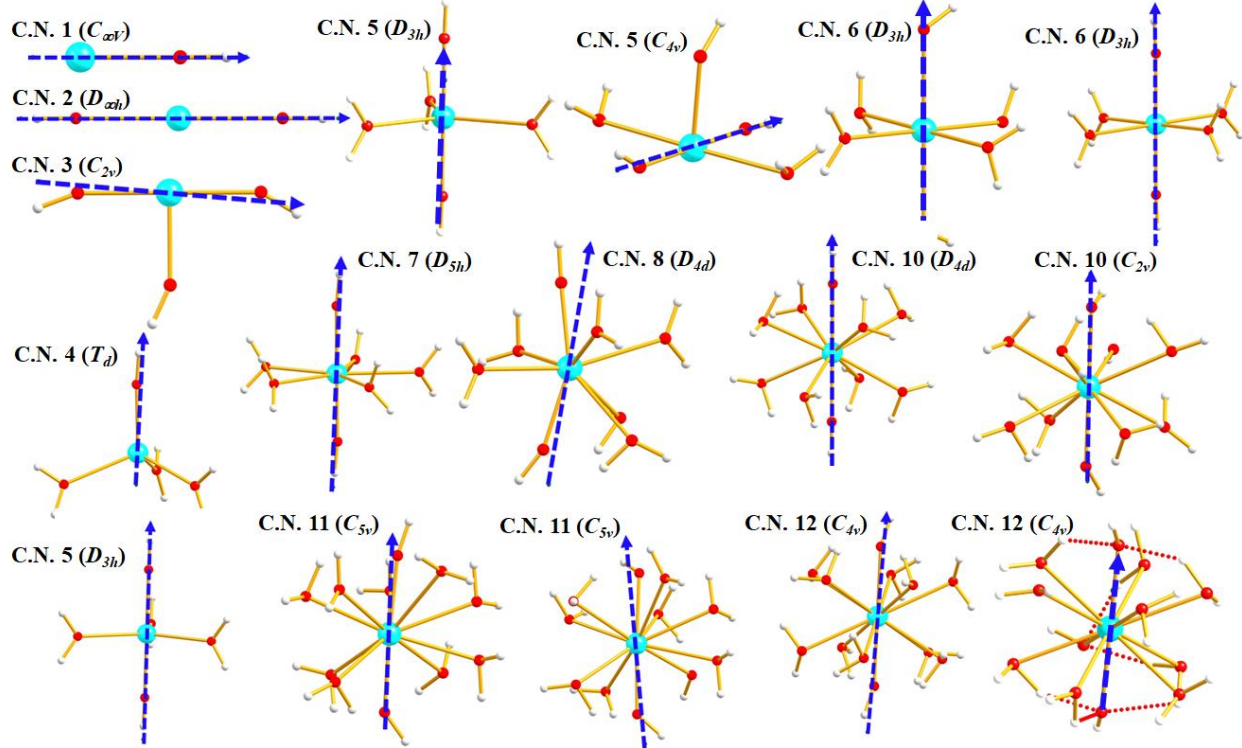


Figure S1: The g_{zz} axis of KD1 of the best performing models from coordination number one to twelve. Colour code: U-cyan, O-red, H-white.

Table S1: The best performing models from coordination number 1 to 12 with estimated U_{cal} values, symmetry, ground state m_J , axial crystal field (CF) parameter B_2^0 and deviation from the ideal geometry (CShM, continuous shape measurement). The CF parameters have been computed according to Stevens Hamiltonian¹³:

$$\hat{H}_{CF} = \sum_{k=2,4,6} \sum_{q=-k}^k B_k^q \tilde{\sigma}_k^q$$

where, B_k^q and $\tilde{\sigma}_k^q$ represent the CF parameter and Stevens operator, respectively.

The CShM analysis was performed in SHAPE v2.1.

C.N .	Model	Geometry	Point Group	U_{cal} (cm ⁻¹)	m_J composition of ground KD	B_2^0	CShM
1	[U(OH) ⁺²	Linear	$C_{\infty v}$	785.4	1.00 ±9/2>	-1.47E+01	0.0
2	[U(OH) ₂] ⁺	Linear	$D_{\infty h}$	976.1	0.99 ±9/2>	-1.68E+01	0.0
3	[U(OH) ₃]	T-shape	C_{2v}	1521.4	0.70 ±5/2>+0.27 ±7/2>	-2.44E+00	0.0
4	[U(OH)(OH ₂) ₃] ²⁺	Tetrahedral	T_d	248.1	0.96 ±9/2>+0.04 ±3/2>	-8.45E+00	0.393
5	[U(OH) ₃ (OH ₂) ₂]*	Trigonal bipyramidal	D_{3h}	596.5	0.95 ±9/2>+0.03 ±5/2>	-1.70E+01	0.723
5	[U(OH) ₂ (OH ₂) ₃] ⁺	Trigonal bipyramidal	D_{3h}	1332.3	1.00 ±9/2>	-2.32E+01	0.723
5	[U(OH) ₃ (OH ₂) ₂]	Vacant octahedron	C_{4v}	1066.0	0.89 ±9/2>+0.10 ±5/2>	-1.71E+01	0.793
6	[U(OH) ₂ (OH ₂) ₄] ⁺	Octahedron	D_{4h}	663.3	0.98 ±9/2>	-1.71E+01	0.730

6	[U(OH) ₃ (OH ₂) ₃]	Octahedron	<i>D</i> _{3h}	223.1	0.91 ±9/2>+0.07 ±1/2>	-8.19E+00	0.079
7	[U(OH) ₂ (OH ₂) ₅] ⁺	Pentagonal bipyramidal	<i>D</i> _{5h}	963.6	1.00 ±9/2>	-1.61E+01	0.592
8	[U(OH) ₂ (OH ₂) ₆] ⁺	square antiprismatic	<i>D</i> _{4d}	653.8	0.95 ±9/2>+0.02 ±7/2>	-1.52E+01	1.638
10	[U(OH) ₂ (OH ₂) ₈] ⁺	Bicapped square antiprism	<i>D</i> _{4d}	1128.3	0.99 ±7/2>	3.70E+00	4.861
10	[U(OH) ₃ (OH ₂) ₇]	Sphenocorona	<i>C</i> _{2v}	924.1	0.93 ±7/2>	6.12E+00	4.370
11	[U(OH) ₂ (OH ₂) ₉] ⁺	Capped pentagonal antiprism J11	<i>C</i> _{5v}	898.0	0.54 ±7/2>+0.40 ±9/2>	-6.67E+00	4.207
11	[U(OH) ₃ (OH ₂) ₈]	Capped pentagonal antiprism J11	<i>C</i> _{5v}	1564.5	0.62 ±7/2>+0.17 ±9/2>+0.14 ±5/2>	-7.82E+00	4.413
12	[U(OH) ₂ (OH ₂) ₁₀] ⁺	icosahedron	<i>C</i> _{4v}	820.6	0.72 ±9/2>+0.20 ±7/2>	-1.11E+01	0.387
12	[U(OH) ₃ (OH ₂) ₉]*	icosahedron	<i>C</i> _{4v}	850.6	0.71 ±7/2>+0.17 ±9/2>+0.05 ±5/2>	2.48E+00	0.387

Table S2: The CASSCF/CASPT2/RASSI-SO/SINGLE_ANISO computed energy of the five ground KDs of $[U(OH)]^{2+}$ along with the g tensor and m_J composition (see Figure S1 for the g_{zz} axis of KD1).

Energy (cm ⁻¹)	g_x	g_y	g_z	m_J composition of the KDs
0.0	0.018	0.018	6.747	$1.00 \pm 9/2\rangle$
509.1	0.012	0.033	5.270	$0.99 \pm 7/2\rangle$
785.4	3.866	3.648	0.806	$0.96 \pm 1/2\rangle$
794.7	0.290	0.356	3.563	$0.96 \pm 5/2\rangle$
969.6	0.279	0.359	2.569	$0.99 \pm 3/2\rangle$

Table S3: The CASSCF/CASPT2/RASSI-SO/SINGLE_ANISO computed energy of the five ground KDs of $[U(OH)_2]^+$ along with the g tensor and m_J composition (see Figure S1 for the g_{zz} axis of KD1).

Energy (cm ⁻¹)	g_x	g_y	g_z	m_J composition of the KDs
0.00	0.016	0.017	6.633	$0.99 \pm 9/2\rangle$
976.1	1.084	1.103	5.023	$0.96 \pm 7/2\rangle + 0.04 \pm 5/2\rangle$
998.5	1.079	1.116	3.368	$0.96 \pm 5/2\rangle + 0.03 \pm 7/2\rangle$
1046.8	3.837	3.696	0.771	$0.99 \pm 1/2\rangle$
1138.5	0.069	0.072	2.371	$0.99 \pm 3/2\rangle$

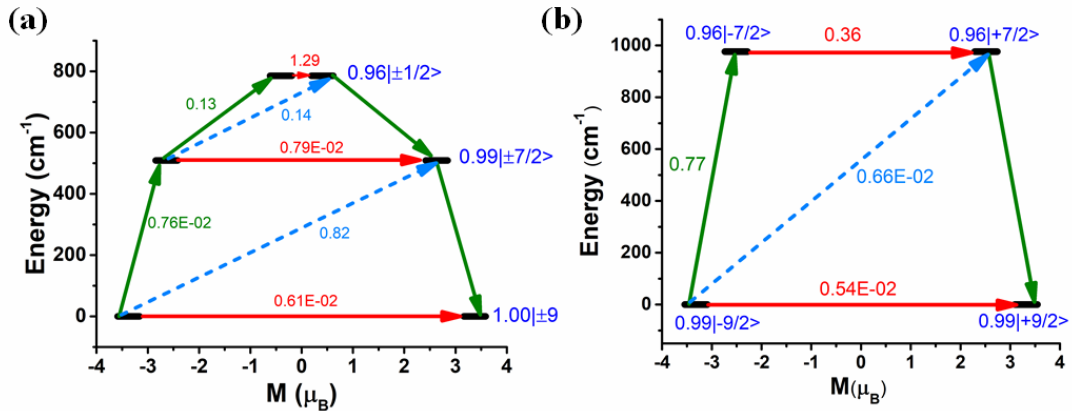


Figure S2: The mechanism of magnetic relaxation (a) $[U(OH)]^{2+}$ (b) $[U(OH)_2]^+$. The black line indicates the KDs as a function of magnetic moments. The red line indicates QTM via ground states and TA-OTM via excited states. The olive line indicates the mechanism of magnetic relaxation. The dashed cyan line indicates a possible Orbach process. The m_J contribution to the KDs is shown by the blue numbers.

Table S4: The CASSCF/RASSI-SO/SINGLE_ANISO computed energy of the five ground KDs of pseudo trigonal pyramidal $[\text{U}(\text{OH})_3]$ along with the g tensor and m_J composition of KD1.

Energy (cm ⁻¹)	g_x	g_y	g_z	m_J composition
0.0	0.639	2.063	5.051	$0.65 \pm 9/2> + 0.21 \pm 5/2> + 0.06 \pm 1/2>$
216.9	2.064	1.733	1.053	
511.9	2.658	2.149	1.475	
993.4	1.830	1.930	4.061	
1248.4	0.049	0.068	6.426	

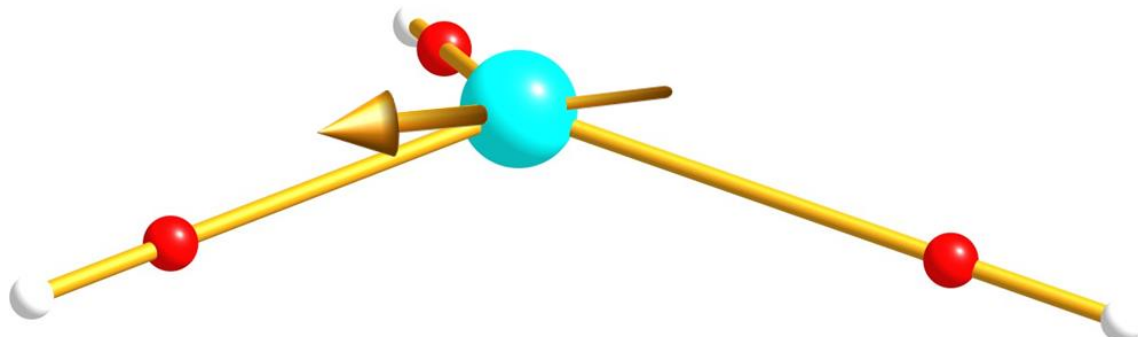


Figure S3: The g_{zz} axis of KD1 of pseudo trigonal pyramidal $[\text{U}(\text{OH})_3]$. This has been modelled from $[\text{U}\{\text{N}(\text{SiMe}_3)_2\}_3]$ (**3**).¹⁴ Colour code: U-cyan, O-red and H-white.

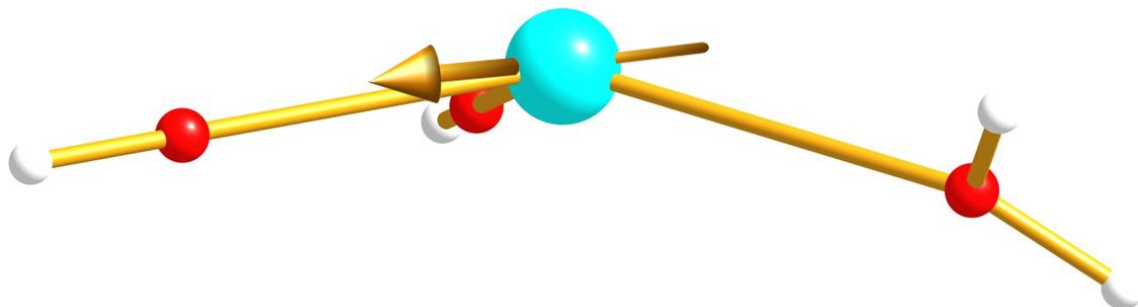


Figure S4: The g_{zz} axis of KD1 of pseudo trigonal pyramidal $[\text{U}(\text{OH})_2(\text{OH}_2)]^+$. This has been modelled from complex $[\text{U}\{\text{N}(\text{SiMe}_3)_2\}_3]$ (**3**).¹⁴ Colour code: U-cyan, O-red and H-white.

Table S5: The CASSCF/RASSI-SO/SINGLE_ANISO computed energy of the five ground KDs of pseudo trigonal pyramidal $[\text{U}(\text{OH})_2(\text{OH}_2)]^+$ along with the g tensor and m_J composition of KD1.

Energy (cm ⁻¹)	g_x	g_y	g_z	m_J composition
0.0	0.646	2.043	4.792	$0.66 \pm 9/2> + 0.17 \pm 5/2> + 0.07 \pm 1/2>$
195.2	0.165	1.657	3.225	
525.1	0.772	1.829	3.939	
795.9	0.818	0.945	4.650	
1046.9	0.036	0.050	6.166	

Table S6: The CASSCF/RASSI-SO/SINGLE_ANISO computed energy of the five ground KDs of pseudo trigonal planar $[\text{U}(\text{OH})_3]$ along with the g tensor and m_J composition of KD1.

Energy (cm^{-1})	g_x	g_y	g_z	m_J composition
0.0	3.633	3.613	0.774	$1.00 \pm 1/2\rangle$
204.1	0.011	0.014	2.216	
527.9	1.786	1.791	2.720	
1080.5	1.852	1.854	4.130	
1355.4	0.000	0.001	6.483	

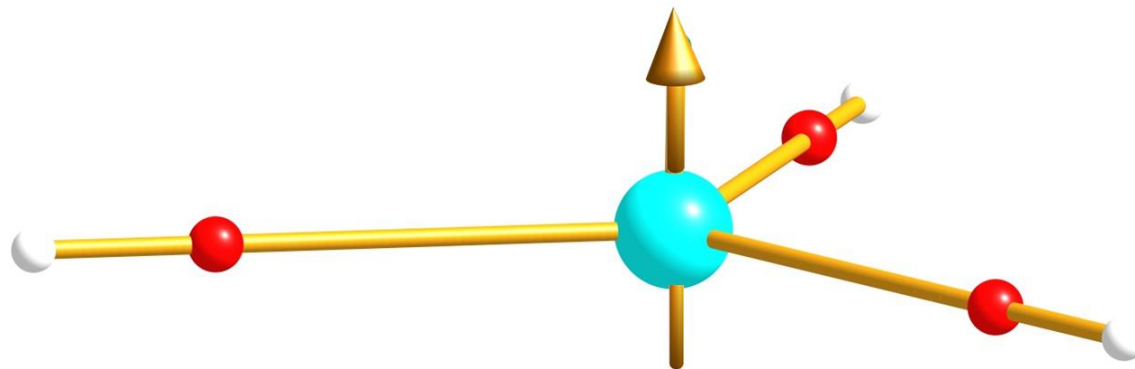


Figure S5: The g_{zz} axis of KD1 of pseudo trigonal planar $[\text{U}(\text{OH})_3]$. This has been modelled from $[\text{U}\{\text{N}(\text{SiMe}_2^t\text{Bu})_2\}_3]$ (2).¹⁵ Colour code: U-cyan, O-red and H-white.

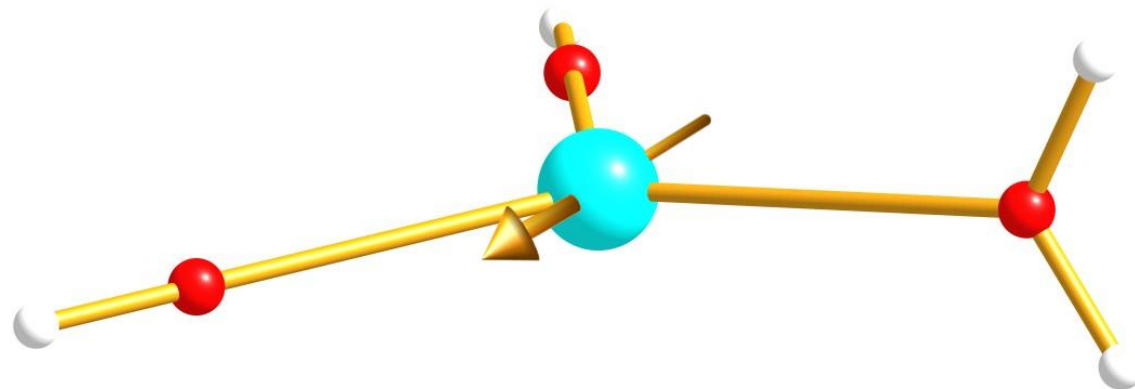


Figure S6: The g_{zz} axis of KD1 of pseudo trigonal planar $[\text{U}(\text{OH})_2(\text{OH}_2)]^+$. This has been modelled from $[\text{U}\{\text{N}(\text{SiMe}_2^t\text{Bu})_2\}_3]$ (2).¹⁵ Colour code: U-cyan, O-red and H-white.

Table S7: The CASSCF/RASSI-SO/SINGLE_ANISO computed energy of the five ground KDs of pseudo trigonal planar $[\text{U}(\text{OH})_2(\text{OH}_2)]^+$ along with the g tensor and m_J composition of KD1.

Energy (cm^{-1})	g_x	g_y	g_z	m_J composition
0.0	0.772	2.505	4.595	$0.71 \pm 9/2\rangle + 0.11 \pm 5/2\rangle + 0.08 \pm 3/2\rangle$
248.9	2.593	1.937	0.598	
700.7	3.173	2.814	0.449	
982.4	1.295	1.521	4.484	
1273.0	0.093	0.123	6.520	

Table S8: The CASSCF/CASPT2/RASSI-SO/SINGLE_ANISO computed energy of the five ground KDs of T-shape $[\text{U}(\text{OH})_3]$ along with the g tensor and m_J composition (see Figure S1 for the g_{zz} axis of KD1) and g_{zz} angle.

Energy (cm ⁻¹)	g_x	g_y	g_z	m_J composition of the KD	Angle of g_{zz} between ground and excited KDs (°)
0.00	0.004	0.014	4.586	$0.70 \pm 5/2> + 0.27 \pm 7/2>$	
592.5	0.020	0.024	5.465	$0.70 \pm 7/2> + 0.27 \pm 5/2>$	4.967
1521.4	0.086	0.420	3.961	$0.62 \pm 1/2> + 0.35 \pm 9/2>$	8.352
1838.8	0.070	0.443	3.600	$0.93 \pm 3/2> + 0.03 \pm 5/2>$	0.994
1890.1	0.080	0.088	2.371	$0.61 \pm 9/2> + 0.36 \pm 1/2>$	0.669

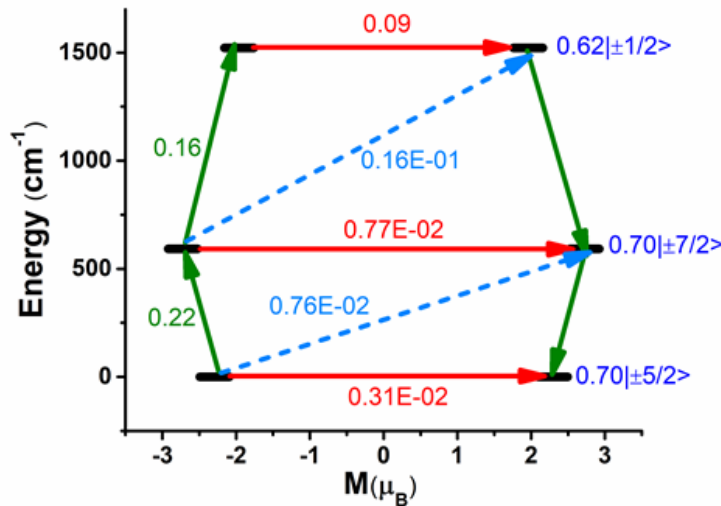


Figure S7: The mechanism of magnetic relaxation $[\text{U}(\text{OH})_3]$. See Figure S2 for colour description.

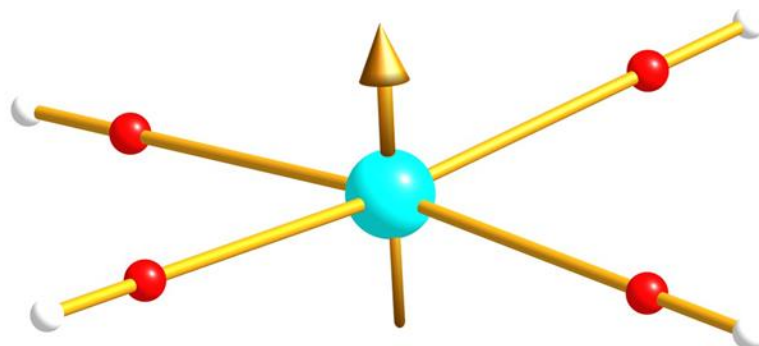


Figure S8: The g_{zz} axis of KD1 of pseudo square planar $[\text{U}(\text{OH})_4]^-$. Colour code: U-cyan, O-red and H-white.

Table S9: The CASSCF/RASSI-SO/SINGLE_ANISO computed energy of the five ground KDs of pseudo square planar $[\text{U}(\text{OH})_4]^-$ along with the g tensor and m_J composition of KD1.

Energy (cm ⁻¹)	g_x	g_y	g_z	m_J composition
0.0	3.963	3.133	0.761	$0.99 \pm 1/2>$
234.5	1.548	1.732	2.318	
823.3	1.768	2.159	3.224	
1228.3	0.016	0.326	5.200	
1597.6	0.140	0.145	6.638	

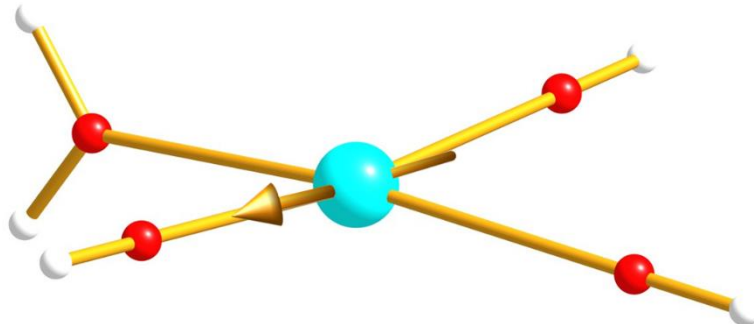


Figure S9: The g_{zz} axis of KD1 of pseudo square planar $[\text{U}(\text{OH})_3(\text{OH}_2)]$. Colour code: U-cyan, O-red and H-white.

Table S10: The CASSCF/RASSI-SO/SINGLE_ANISO computed energy of the five ground KDs of pseudo square planar $[\text{U}(\text{OH})_3(\text{OH}_2)]$ along with the g tensor and m_J composition of KD1.

Energy (cm ⁻¹)	g_x	g_y	g_z	m_J composition
0.0	0.079	2.333	4.623	$0.69 \pm 9/2>+0.15 \pm 5/2>+0.05 \pm 1/2>$
315.1	0.871	1.677	3.102	
985.5	3.069	2.724	0.475	
1310.0	1.186	1.388	4.537	
1629.8	0.128	0.195	6.549	

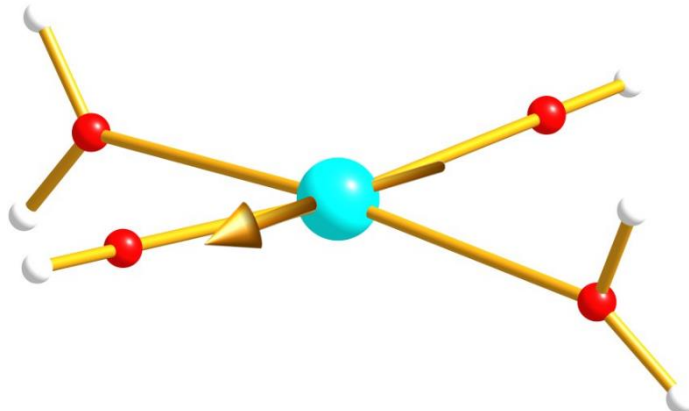


Figure S10: The g_{zz} axis of KD1 of pseudo square planar trans- $[\text{U}(\text{OH})_2(\text{OH}_2)_2]^+$. Colour code: U-cyan, O-red and H-white.

Table S11: The CASSCF/RASSI-SO/SINGLE_ANISO computed energy of the five ground KDs of pseudo square planar trans-[U(OH)₂(OH₂)₂]⁺ along with the g tensor and m_J composition of KD1.

Energy (cm ⁻¹)	g _x	g _y	g _z	m _J composition
0.0	0.440	0.765	5.961	0.91 ±9/2>+0.06 ±5/2>+0.03 ±3/2>
472.7	0.539	1.400	4.568	
1037.9	0.670	1.777	3.398	
1328.3	1.754	2.243	3.490	
1552.3	0.251	0.439	6.427	

Table S12: The CASSCF/RASSI-SO/SINGLE_ANISO computed energy of the five ground KDs of pseudo square planar cis-[U(OH)₂(OH₂)₂]⁺ along with the g tensor and m_J composition of KD1.

Energy (cm ⁻¹)	g _x	g _y	g _z	m _J composition
0.0	3.663	3.274	0.788	0.98 ±1/2>
226.6	2.717	2.256	1.196	
941.8	0.541	1.245	4.424	
1122.1	1.424	2.270	4.072	
1416.2	0.103	0.192	6.494	

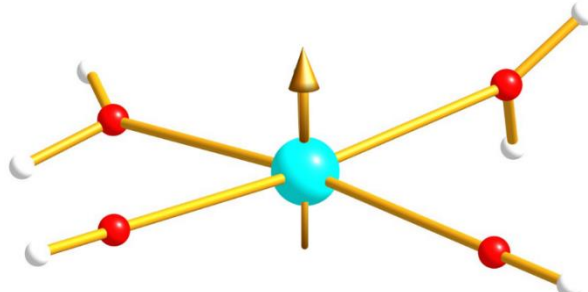


Figure S11: The g_{zz} axis of KD1 of pseudo square planar cis-[U(OH)₂(OH₂)₂]⁺. Colour code: U-cyan, O-red and H-white.

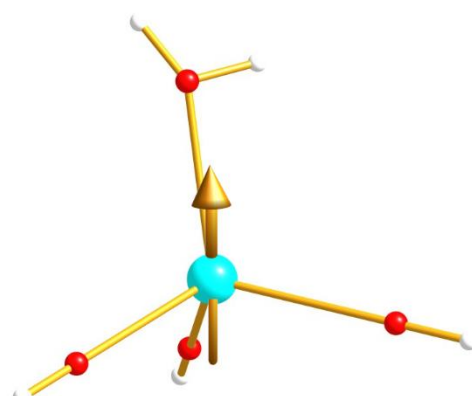


Figure S12: The g_{zz} axis of KD1 of pseudo tetrahedral [U(OH)₃(OH₂)]. It has been modelled from [U(OSi(O'Bu)₃)₄]⁻ (6).¹⁶ Colour code: U-cyan, O-red and H-white.

Table S13: The CASSCF/RASSI-SO/SINGLE_ANISO computed energy of the five ground KDs of pseudo tetrahedral $[\text{U(OH)}_3(\text{OH}_2)]$ along with the g tensor and m_J composition of KD1.

Energy (cm^{-1})	g_x	g_y	g_z	m_J composition
0.0	0.504	0.934	5.427	$0.70 +9/2>+0.25 +5/2>$
138.8	3.208	2.342	1.073	
293.5	2.694	2.002	0.508	
465.7	0.028	1.742	3.611	
637.9	0.996	1.820	4.713	

Table S14: The CASSCF/CASPT2/RASSI-SO/SINGLE_ANISO computed energy of the five ground KDs along with the g tensor and decomposition of m_J states of pseudo tetrahedral $[\text{U(OH)}(\text{OH}_2)_3]^{2+}$ (see Figure S1 for the g_{zz} axis of KD1). The $[\text{U(OH)}(\text{OH}_2)_3]^{2+}$ has been modelled from complex **6**.¹⁶

Energy (cm^{-1})	g_x	g_y	g_z	m_J decomposition of the KDs
0.00	0.010	0.033	6.476	$0.96 +9/2>+0.04 +3/2>$
248.07	0.619	0.781	4.699	$0.85 -7/2>+0.12 +1/2>$
432.56	1.002	1.694	3.646	$0.78 -1/2>+0.13 -7/2>$
569.57	0.864	2.446	4.059	$0.50 +5/2>+0.39 +3/2>$
663.30	3.545	3.137	0.064	$0.52 -3/2>+0.45 +5/2>$

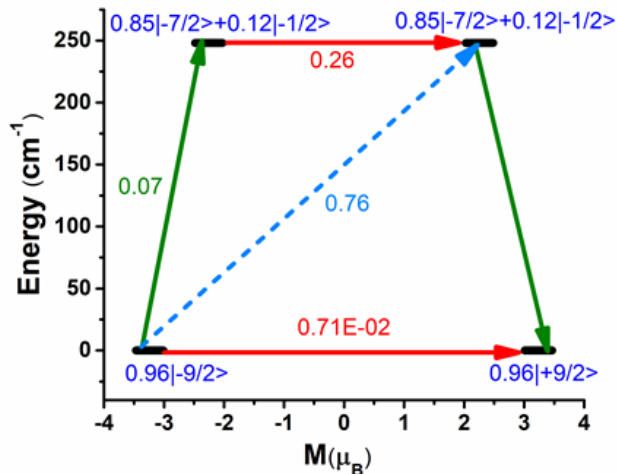


Figure S13: The mechanism of magnetic relaxation pseudo tetrahedral $[\text{U(OH)}(\text{OH}_2)_3]^{2+}$. See Figure S2 for colour description.

Table S15: The CASSCF/RASSI-SO/SINGLE_ANISO computed energy of the five ground KDs of pseudo trigonal bipyramidal $[\text{U}(\text{OH})_3(\text{OH}_2)_2]$ (model 1) along with the g tensor and m_J composition of KD1.

Energy (cm ⁻¹)	g_x	g_y	g_z	m_J composition
0.0	0.848	2.212	4.186	$0.58 \pm 9/2> + 0.19 \pm 5/2> + 0.10 \pm 3/2>$
85.9	0.534	1.973	3.607	
370.2	3.524	2.842	0.630	
503.1	0.080	0.854	4.529	
798.5	0.458	0.749	5.275	

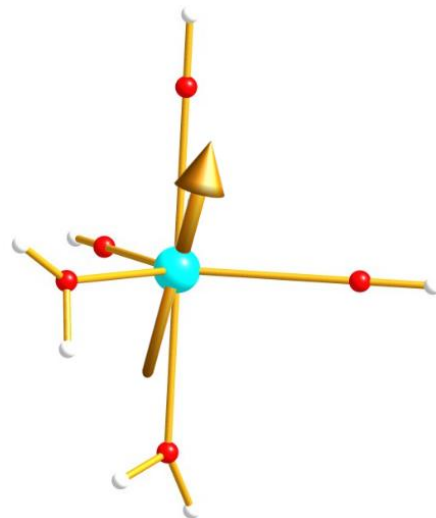


Figure S14: The g_{zz} axis of KD1 of pseudo trigonal bipyramidal $[\text{U}(\text{OH})_3(\text{OH}_2)_2]$ (model 1). It has been modelled from $[\text{UN}^*_3(\text{CN})_2]^+$ (**8**, $\text{N}^* = \text{N}(\text{SiMe}_3)_2$).¹⁷ Colour code: U-cyan, O-red and H-white.

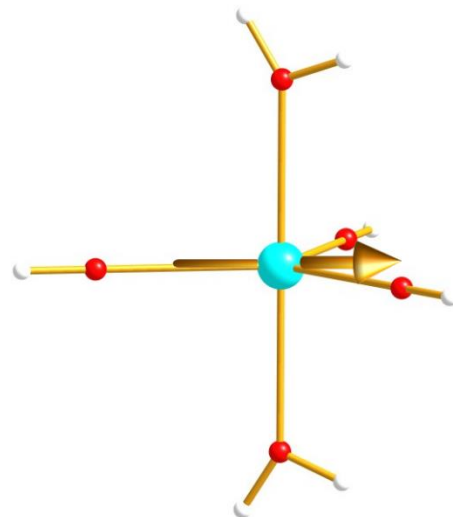


Figure S15: The g_{zz} axis of KD1 of pseudo trigonal bipyramidal $[\text{U}(\text{OH})_3(\text{OH}_2)_2]$ (model 2). It has been modelled from $[\text{UN}^*_3(\text{CN})_2]^+$ (**8**, $\text{N}^* = \text{N}(\text{SiMe}_3)_2$).¹⁷ Colour code: U-cyan, O-red and H-white.

Table S16: The CASSCF/RASSI-SO/SINGLE_ANISO computed energy of the five ground KDs of pseudo trigonal bipyramidal $[\text{U}(\text{OH})_3(\text{OH}_2)_2]$ (model 2) along with the g tensor and m_J composition of KD1.

Energy (cm^{-1})	g_x	g_y	g_z	m_J composition
0.0	1.182	1.487	2.462	$0.38 \pm 7/2> + 0.25 \pm 1/2> + 0.24 \pm 9/2> + 0.11 \pm 3/2>$
113.9	0.684	1.174	4.609	
169.8	2.776	2.643	0.283	
426.2	0.097	0.446	5.491	
892.7	1.321	1.758	4.495	

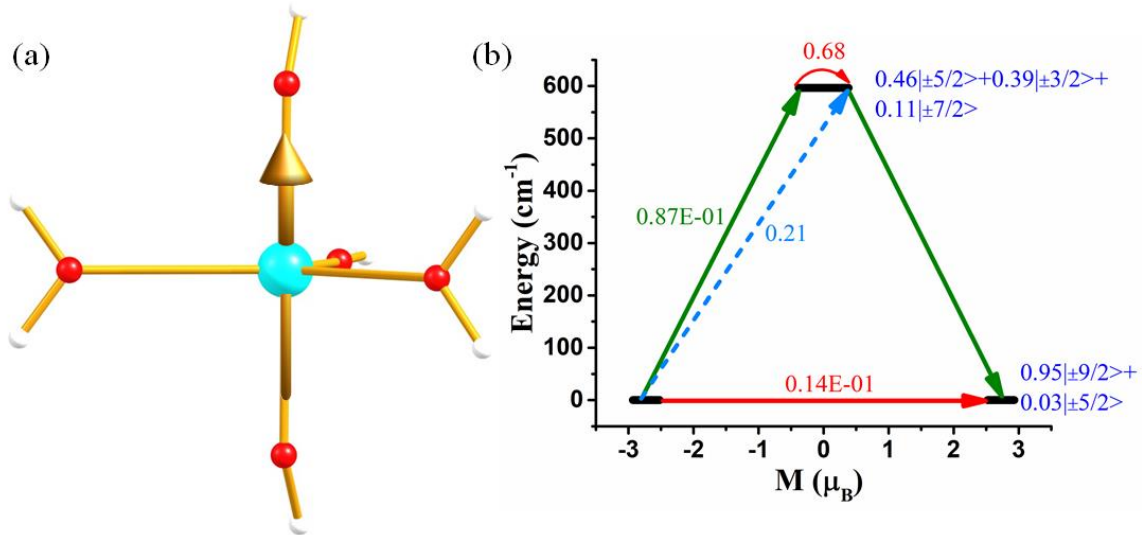


Figure S16: (a) The g_{zz} axis of KD1 of pseudo trigonal bipyramidal $[\text{U}(\text{OH})_3(\text{OH}_2)_2]$ (model 3). It has been modelled from $[\text{UN}^*_3(\text{CN})_2]^+$ (**8**, $\text{N}^* = \text{N}(\text{SiMe}_3)_2$).¹⁷ Colour code: U-cyan, O-red and H-white. (b) The mechanism of magnetic relaxation of pseudo trigonal bipyramidal $[\text{U}(\text{OH})_3(\text{OH}_2)_2]$ (model 3). See Figure S2 for colour description.

Table S17: The CASSCF/CASPT2/RASSI-SO/SINGLE_ANISO computed energy of the five ground KDs of pseudo trigonal bipyramidal $[\text{U}(\text{OH})_3(\text{OH}_2)_2]$ (model 3) along with the g tensor and m_J composition of KD1.

Energy (cm^{-1})	g_x	g_y	g_z	m_J composition
0.0	0.033	0.049	5.450	$0.95 \pm 9/2> + 0.03 \pm 5/2>$
596.5	0.257	0.355	3.779	
1424.2	0.125	0.305	5.972	
1965.0	0.291	0.445	4.872	
2212.8	1.343	1.785	3.928	

Table S18: The CASSCF/CASPT2/RASSI-SO/SINGLE_ANISO computed energy of the five ground KDs of pseudo trigonal bipyramidal $[\text{U}(\text{OH})_2(\text{OH}_2)_3]^+$ along with the g tensor and m_J composition (see Figure S1 for the g_{zz} axis of KD1, modelled from complex **8**¹⁷)

Energy (cm^{-1})	g_x	g_y	g_z	m_J composition of the KDs
0.00	0.000	0.001	6.091	$1.00 \pm 9/2>$
1332.3	2.611	2.265	0.707	$0.68 \pm 5/2> + 0.32 \pm 7/2>$

1464.2	0.119	0.235	1.623	0.97 ±3/2>
1573.7	2.909	2.451	1.625	0.66 ±7/2>+0.32 ±5/2>
1598.1	3.593	3.120	0.607	0.96 ±1/2>

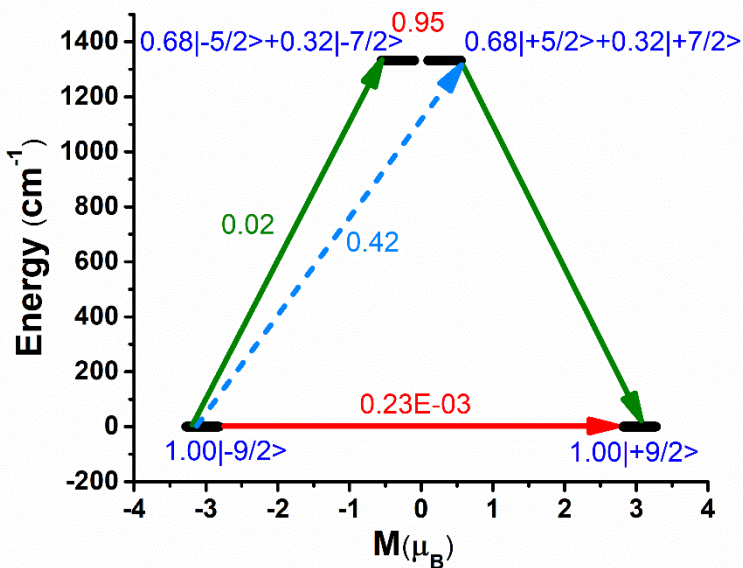


Figure S17: The mechanism of magnetic relaxation of pseudo trigonal bipyramidal $[\text{U}(\text{OH})_2(\text{OH}_2)_3]^+$. See Figure S2 for colour description.

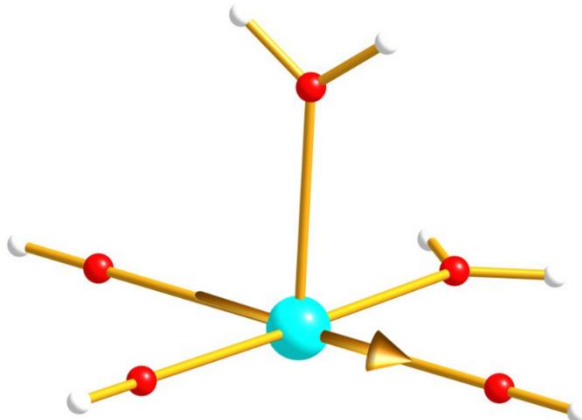


Figure S18: The g_{zz} axis of KD1 of pseudo square pyramidal $[\text{U}(\text{OH})_3(\text{OH}_2)_2]$ (model 1). Colour code: U-cyan, O-red and H-white.

Table S19: The CASSCF/RASSI-SO/SINGLE_ANISO computed energy of the five ground KDs of pseudo square pyramidal $[\text{U}(\text{OH})_3(\text{OH}_2)_2]$ (model 1) along with the g tensor and m_J composition of KD1.

Energy (cm⁻¹)	g_x	g_y	g_z	m_J composition
0.0	0.422	0.838	5.806	0.88 ±9/2>+0.08 ±5/2>
220.5	0.033	0.798	5.239	
702.6	0.076	0.988	4.141	
1023.1	2.668	2.248	1.558	
1097.9	0.517	0.868	4.669	

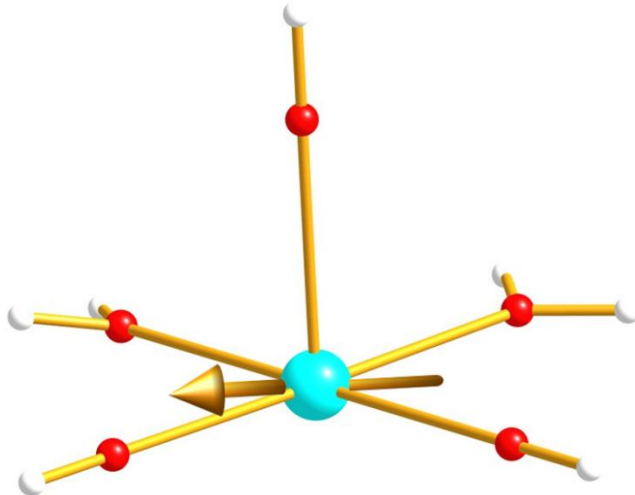


Figure S19: The g_{zz} axis of KD1 of pseudo square pyramidal $[\text{U}(\text{OH})_3(\text{OH}_2)_2]$ (model 2). Colour code: U-cyan, O-red and H-white.

Table S20: The CASSCF/RASSI-SO/SINGLE_ANISO computed energy of the five ground KDs of pseudo square pyramidal $[\text{U}(\text{OH})_3(\text{OH}_2)_2]$ (model 2) along with the g tensor and m_J composition of KD1.

Energy (cm^{-1})	g_x	g_y	g_z	m_J composition
0.0	0.309	1.700	3.879	$0.42 9/2>+0.34 5/2>+0.17 1/2>$
100.2	0.235	1.495	3.495	
419.7	3.340	2.732	0.036	
618.5	0.860	1.457	4.837	
833.8	1.383	1.483	4.345	

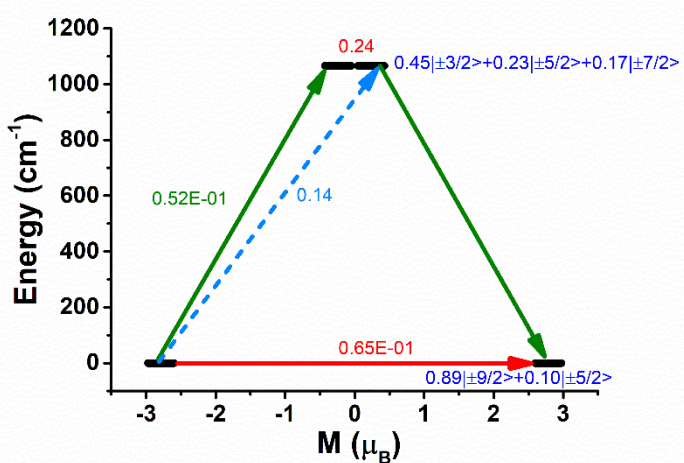


Figure S20: The mechanism of magnetic relaxation of pseudo square pyramidal $[\text{U}(\text{OH})_3(\text{OH}_2)_2]$ (model 3, see Figure S1 for the g_{zz} axis of KD1). See Figure S2 for colour description.

Table S21: The CASSCF/CASPT2/RASSI-SO/SINGLE_ANISO computed energy of the five ground KDs along with the g tensor and decomposition of m_J states of pseudo square pyramidal $[\text{U}(\text{OH})_3(\text{OH}_2)_2]$ (model 3)

Energy (cm ⁻¹)	g_x	g_y	g_z	m_J decomposition of the KDs
0.00	0.167	0.225	5.569	$0.89 \pm 9/2> + 0.10 \pm 5/2>$
1066.0	0.591	0.808	4.059	$0.45 \pm 3/2> + 0.23 \pm 5/2> + 0.12 \pm 1/2>$
1336.2	0.535	1.771	4.093	$0.43 \pm 3/2> + 0.31 \pm 5/2> + 0.07 \pm 9/2>$
1526.4	2.562	2.478	0.621	$0.56 \pm 1/2> + 0.22 \pm 7/2> + 0.18 \pm 5/2>$
2231.4	2.228	2.364	2.618	$0.57 \pm 7/2> + 0.18 \pm 5/2> + 0.15 \pm 1/2>$

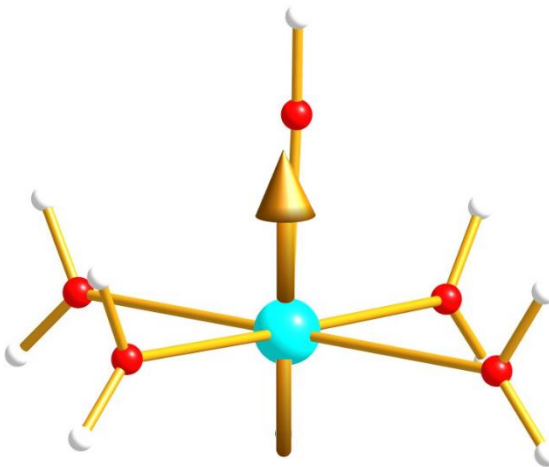


Figure S21: The g_{zz} axis of KD1 of pseudo square pyramidal $[\text{U}(\text{OH})(\text{OH}_2)_4]^{2+}$. Colour code: U-cyan, O-red and H-white.

Table S22: The CASSCF/CASPT2/RASSI-SO/SINGLE_ANISO computed energy of the five ground KDs of pseudo square pyramidal $[\text{U}(\text{OH})(\text{OH}_2)_4]^{2+}$ along with the g tensor and m_J composition of KD1.

Energy (cm ⁻¹)	g_x	g_y	g_z	m_J composition
0.0	3.042	2.871	1.046	$0.90 \pm 1/2> + 0.06 \pm 9/2>$
133.9	0.658	0.589	4.521	
286.1	0.093	0.453	5.641	
314.0	3.312	2.735	0.691	
714.6	3.454	3.292	0.481	

Table S23: The CASSCF/CASPT2/RASSI-SO/SINGLE_ANISO computed energy of the five ground KDs of pseudo-octahedral fac-[U(OH)₃(OH₂)₃] along with the g tensor and m_J composition of KD1.

Energy (cm ⁻¹)	g_x	g_y	g_z	m_J composition
0.0	1.095	1.375	3.473	$0.49 \pm 3/2> + 0.37 \pm 9/2> + 0.06 \pm 1/2>$
136.5	3.098	1.933	0.241	
304.8	3.639	2.587	0.422	
646.2	1.258	2.333	3.748	
960.7	0.487	0.649	4.743	

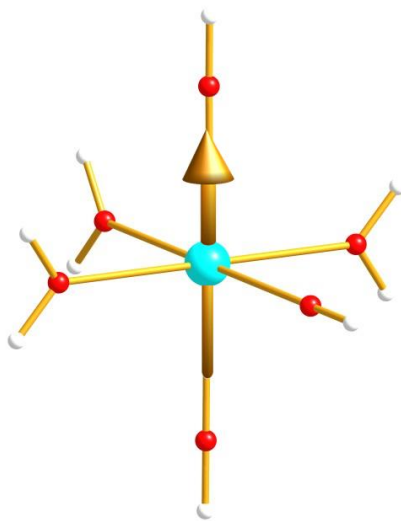


Figure S22: The g_{zz} axis of KD1 of pseudo-octahedral fac-[U(OH)₃(OH₂)₃]. It has been modelled from [UI₂(OPPh₃)₄][I] (**15**).¹⁸ Colour code: U-cyan, O-red and H-white.

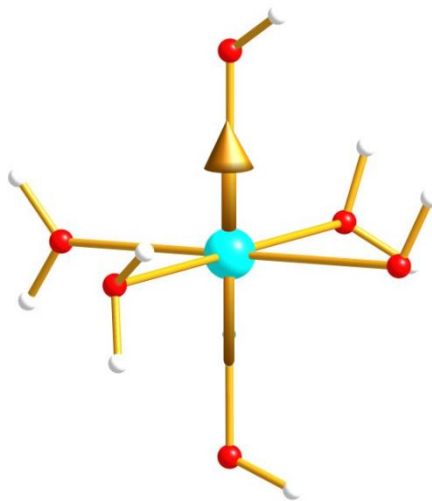


Figure S23: The g_{zz} axis of KD1 of pseudo-octahedral mer-[U(OH)₃(OH₂)₃]. It has been modelled from [UI₂(OPPh₃)₄][I] (**15**).¹⁸ Colour code: U-cyan, O-red and H-white.

Table S24: The CASSCF/CASPT2/RASSI-SO/SINGLE_ANISO computed energy of the five ground KDs of pseudo-octahedral mer-[U(OH)₃(OH₂)₃] (modelled from complex **15**, see Figure S1 for the g_{zz} axis of KD1) along with the g tensor and m_J composition.

Energy (cm ⁻¹)	g_x	g_y	g_z	m_J composition of the KDs
0.00	0.116	0.380	5.909	$0.91 \pm 9/2 > + 0.07 \pm 1/2 >$
223.1	0.499	1.304	5.112	$0.46 3/2 > + 0.40 \pm 5/2 > + 0.04 \pm 9/2 >$
541.4	0.290	1.456	5.194	$0.70 \pm 1/2 > + 0.13 \pm 7/2 > + 0.05 \pm 9/2 >$
898.5	1.352	1.724	3.824	$0.75 \pm 7/2 > + 0.12 \pm 1/2 > + 0.08 \pm 5/2 >$
1365.8	0.492	1.719	4.755	$0.45 \pm 5/2 > + 0.42 \pm 3/2 > + 0.09 \pm 7/2 >$

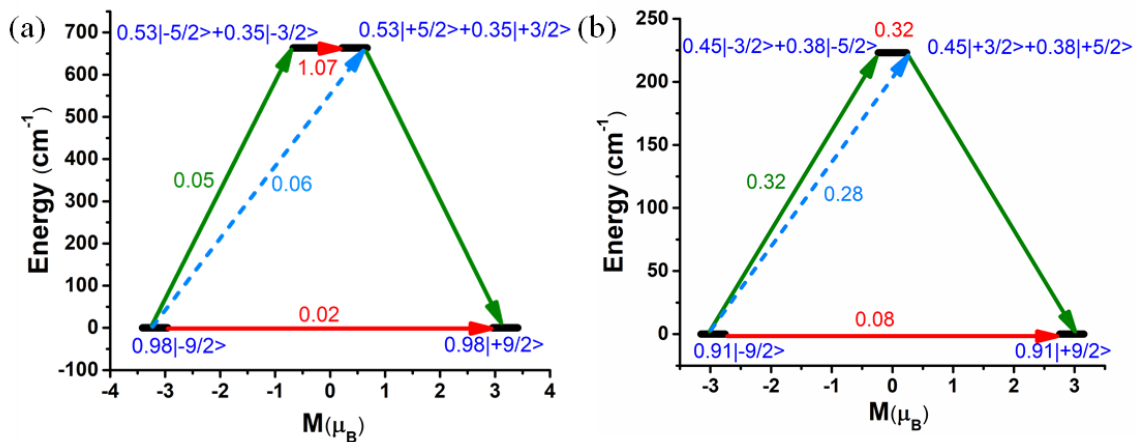


Figure S24: The mechanism of magnetic relaxation (a) pseudo-octahedral $[\text{U}(\text{OH})_2(\text{OH}_2)_4]^+$ (b) pseudo-octahedral $[\text{U}(\text{OH})_3(\text{OH}_2)_3]$. See Figure S2 for colour description.

Table S25: The computed energy of the five ground KDs of pseudo-octahedral $[\text{U}(\text{OH})_2(\text{OH}_2)_4]^+$ (modelled from complex **15**, see Figure S1 for the g_{zz} axis of KD1) along with the g tensor and m_J composition.

Energy (cm^{-1})	g_x	g_y	g_z	m_J decomposition of the KDs
0.00	0.056	0.056	6.370	$0.98 -9/2>$
663.3	3.140	3.002	0.889	$0.53 +5/2>+0.35 +3/2>$
927.9	2.510	2.385	1.359	$0.58 +1/2>+0.40 +7/2>$
1248.8	0.735	0.867	2.693	$0.60 +7/2>+0.39 +1/2>$
1798.6	3.326	3.270	0.535	$0.52 +5/2>+0.47 +5/2>$

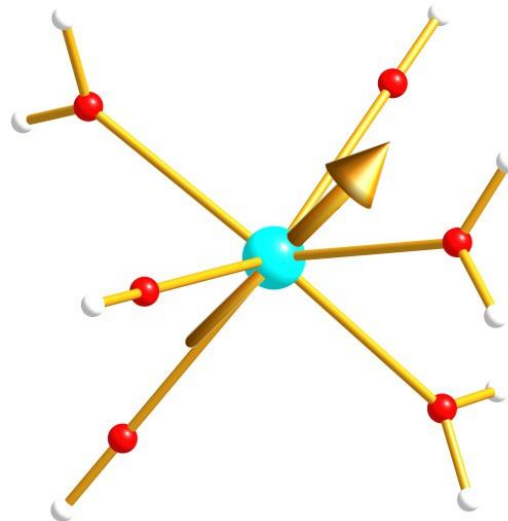


Figure S25: The g_{zz} axis of KD1 of pseudo trigonal prismatic $[\text{U}(\text{OH})_3(\text{OH}_2)_3]$. It has been modelled from $[\text{U}(\text{H}_2\text{BPz}_2)_3]$ (**12**, H_2BPz_2 = dihydrobispypyrazolylborate).¹⁹ Colour code: U-cyan, O-red and H-white.

Table S26: The computed energy of the five ground KDs of pseudo trigonal prismatic $[\text{U}(\text{OH})_3(\text{OH}_2)_3]$ along with the g tensor and m_J composition of KD1.

Energy (cm ⁻¹)	g_x	g_y	g_z	m_J composition
0.0	0.261	0.442	5.873	$0.88 \pm 9/2> + 0.06 \pm 5/2>$
303.6	0.936	1.811	3.585	
373.1	1.367	1.744	3.721	
598.3	0.158	1.821	3.739	
822.7	1.053	1.657	4.851	

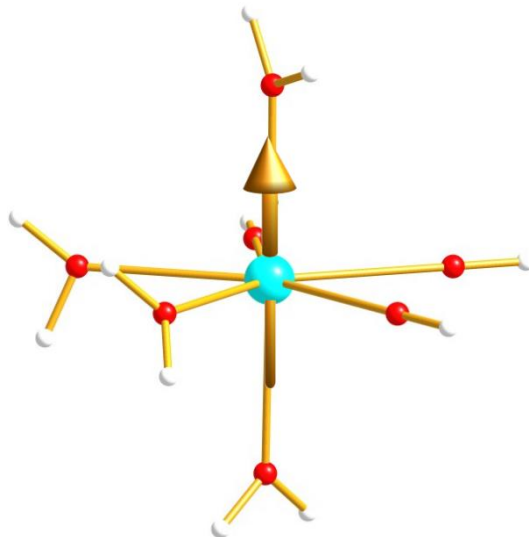


Figure S26: The g_{zz} axis of KD1 of pseudo pentagonal bipyramidal $[\text{U}(\text{OH})_3(\text{OH}_2)_4]$ (model1). It has been modelled from $[\text{UO}_2(\text{NCS})_4(\text{H}_2\text{O})]^{2-}$.²⁰ Colour code: U-cyan, O-red and H-white.

Table S27: The computed energy of the five ground KDs of pseudo pentagonal bipyramidal $[\text{U}(\text{OH})_3(\text{OH}_2)_4]$ (model 1) along with the g tensor and m_J composition of KD1.

Energy (cm ⁻¹)	g_x	g_y	g_z	m_J composition
0.0	3.752	2.936	0.711	$0.96 \pm 1/2>$
185.1	0.311	0.493	1.713	
513.9	2.517	2.037	1.543	
852.2	0.002	0.388	5.672	
1299.5	3.322	2.738	1.872	

Table S28: The computed energy of the five ground KDs of pseudo pentagonal bipyramidal $[\text{U}(\text{OH})_3(\text{OH}_2)_4]$ (model 2) along with the g tensor and m_J composition of KD1.

Energy (cm ⁻¹)	g_x	g_y	g_z	m_J composition
0.0	0.400	1.068	5.737	$0.88 \pm 9/2> + 0.05 \pm 5/2>$
141.2	1.685	1.962	2.486	
504.8	0.226	0.900	3.350	
648.2	0.117	0.127	6.002	
1105.5	0.421	0.906	4.852	

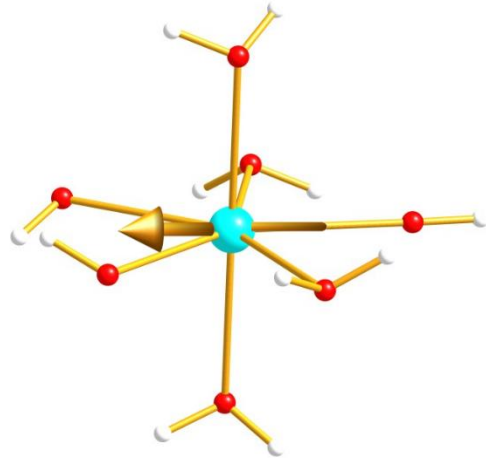


Figure S27: The g_{zz} axis of KD1 of pseudo pentagonal bipyramidal $[\text{U}(\text{OH})_3(\text{OH}_2)_4]$ (model2). It has been modelled from $[\text{UO}_2(\text{NCS})_4(\text{H}_2\text{O})]^{2-}$.²⁰ Colour code: U-cyan, O-red and H-white.

~~Figure S27. The mechanism of magnetic relaxation pseudo pentagonal bipyramidal $[\text{U}(\text{OH})_2(\text{OH}_2)_5]^+$ along with the g tensor and m_J composition (modelled from $[\text{UO}_2(\text{NCS})_4(\text{H}_2\text{O})]^{2-}$, see Figure S1 for the g_{zz} axis of KD1).~~

Energy (cm^{-1})	g_x	g_y	g_z	m_J decomposition of the KDs
0.00	0.005	0.022	6.232	$1.00 \pm 9/2>$
963.6	3.140	3.002	0.889	$0.72 \pm 1/2>+0.22 \pm 3/2>$
1179.4	2.510	2.385	1.359	$0.76 \pm 5/2>+0.13 \pm 1/2>+0.07 \pm 7/2>$
1268.7	0.735	0.867	2.693	$0.40 \pm 7/2>+0.44 \pm 3/2>+0.09 \pm 1/2>$
1356.6	3.326	3.270	0.535	$0.52 \pm 7/2>+0.31 \pm 3/2>+0.06 \pm 1/2>$

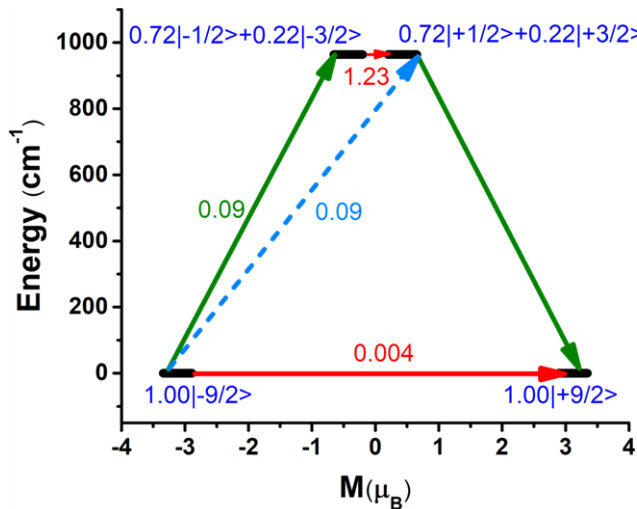


Figure S28: The mechanism of magnetic relaxation pseudo pentagonal bipyramidal $[\text{U}(\text{OH})_2(\text{OH}_2)_5]^+$. See Figure S2 for colour description.

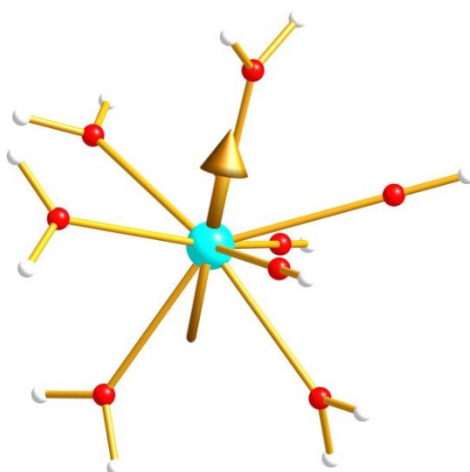


Figure S29: The g_{zz} axis of KD1 of pseudo trigonal prismatic $[\text{U}(\text{OH})_3(\text{OH}_2)_5]$. It has been modelled from $[\text{U}(\text{Tp}^{\text{Me}^2})_2(\text{bipy})]^+$ (**19**, Tp^{Me^2} = hydrotris(3,5-dimethylpyrazolyl)borate).²¹ Colour code: U-cyan, O-red and H-white.

Table S30: The computed energy of the five ground KDs of pseudo trigonal prismatic $[\text{U}(\text{OH})_3(\text{OH}_2)_5]$ along with the g tensor and m_J composition of KD1.

Energy (cm ⁻¹)	g_x	g_y	g_z	m_J composition
0.0	3.654	2.076	0.488	$0.57 \pm 1/2> + 0.19 \pm 3/2> + 0.10 \pm 9/2> + 0.06 \pm 7/2>$
219.8	0.519	1.718	3.288	
416.9	0.386	1.383	3.685	
789.2	2.605	2.333	0.236	
1182.1	1.724	2.393	3.231	

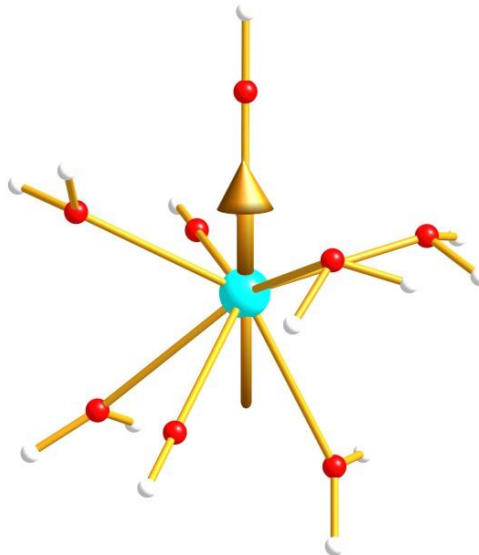


Figure S30: The g_{zz} axis of KD1 of pseudo triangular dodecahedron $[\text{U}(\text{OH})_3(\text{OH}_2)_5]$. It has been modelled from $[\text{UI}_3(\text{Me}^4\text{phen})_2(\text{py})]$ (**20**, Me⁴phen = 3,4,7,8-tetramethyl-1,10-phenanthroline).²² Colour code: U-cyan, O-red and H-white.

Table S31: The computed energy of the five ground KDs of pseudo triangular dodecahedron $[\text{U}(\text{OH})_3(\text{OH}_2)_5]$ along with the g tensor and m_J composition of KD1.

Energy (cm ⁻¹)	g_x	g_y	g_z	m_J composition
0.0	4.048	3.269	0.397	$0.39 \pm 1/2> + 0.24 \pm 5/2> + 0.16 \pm 7/2> + 0.10 \pm 3/2>$
292.8	0.476	2.222	4.022	
502.8	3.614	2.024	0.400	
794.8	3.219	2.569	0.088	
989.9	0.371	1.970	5.434	

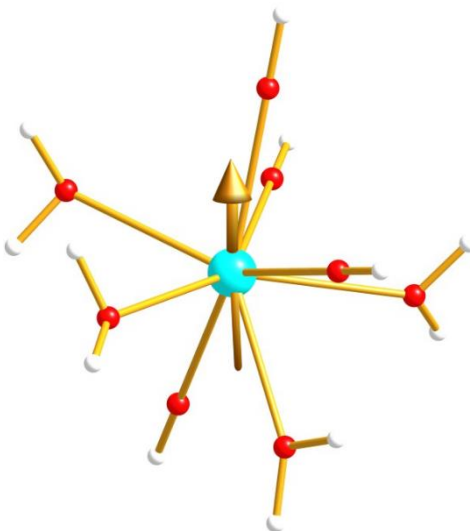


Figure S31: The g_{zz} axis of KD1 of pseudo triangular dodecahedron $[\text{U}(\text{OH})_4(\text{OH}_2)_4]^-$. It has been modelled from $[\text{UI}_3(\text{Me}_4\text{phen})_2(\text{py})]$ (**20**, Me₄phen = 3,4,7,8-tetramethyl-1,10-phenanthroline).²² Colour code: U-cyan, O-red and H-white.

Table S32: The computed energy of the five ground KDs of pseudo triangular dodecahedron $[\text{U}(\text{OH})_4(\text{OH}_2)_4]^-$ along with the g tensor and m_J composition of KD1.

Energy (cm ⁻¹)	g_x	g_y	g_z	m_J composition
0.0	0.494	1.877	4.792	$0.44 \pm 9/2> + 0.44 \pm 3/2> + 0.05 \pm 5/2>$
310.1	0.301	1.332	4.588	
501.1	0.149	2.128	4.721	
780.2	0.266	1.212	3.239	
962.1	1.571	2.106	4.141	

Table S33: The computed energy of the five ground KDs of pseudo square antiprismatic $[\text{U}(\text{OH})_2(\text{OH}_2)_6]^+$ along with the g tensor and m_J composition (see Figure S1 for the g_{zz} axis of KD1, it has been modelled from complex **20**)

Energy (cm ⁻¹)	g_x	g_y	g_z	m_J composition of the KDs
0.00	0.022	0.040	5.726	$0.95 \pm 9/2> + 0.02 \pm 7/2>$
653.8	1.019	1.712	3.642	$0.51 \pm 7/2> + 0.38 \pm 3/2> + 0.06 \pm 1/2>$
957.6	0.237	0.865	4.092	$0.30 \pm 3/2> + 0.29 \pm 7/2> + 0.23 \pm 5/2>$
1282.5	0.070	1.667	3.165	$0.49 \pm 1/2> + 0.21 \pm 7/2> + 0.16 \pm 5/2>$
1724.8	3.328	2.340	0.647	$0.45 \pm 7/2> + 0.24 \pm 1/2> + 0.20 \pm 3/2>$

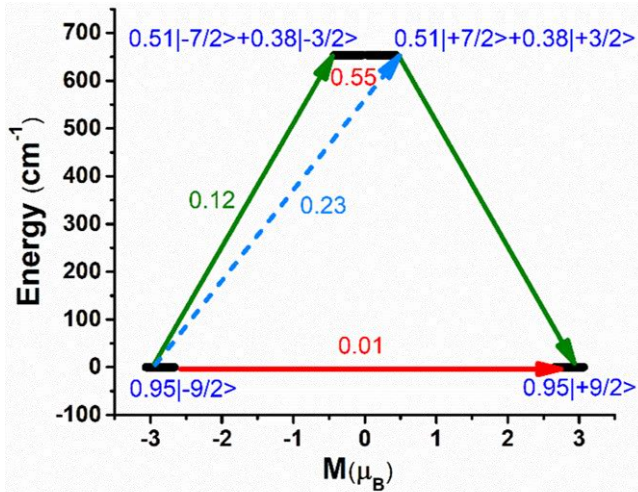


Figure S32: The mechanism of magnetic relaxation of pseudo square antiprismatic $[\text{U}(\text{OH})_2(\text{OH}_2)_6]^+$. See Figure S2 for colour description.

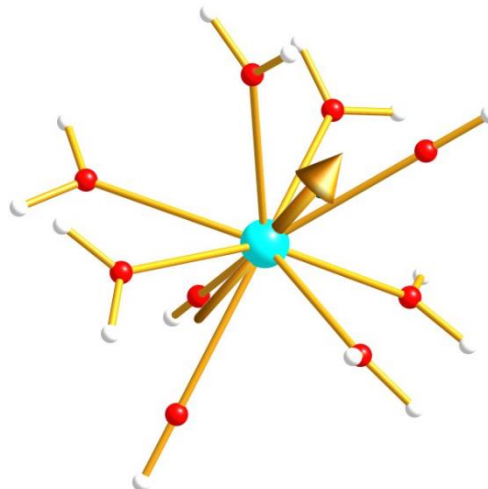


Figure S33: The g_{zz} axis of KD1 of pseudo tricapped trigonal prismatic $[\text{U}(\text{OH})_3(\text{OH}_2)_6]$. It has been modelled from $[\text{U}(\text{terpy})_3]\text{I}_3\cdot 2\text{MeCN}$ (terpy = 2,2':6',2''-terpyridine).²³ Colour code: U-cyan, O-red and H-white.

Table S34: The computed energy of the five ground KDs of pseudo tricapped trigonal prismatic $[\text{U}(\text{OH})_3(\text{OH}_2)_6]$ along with the g tensor and m_J composition of KD1.

Energy (cm ⁻¹)	g_x	g_y	g_z	m_J composition
0.0	0.382	0.692	5.381	$0.84 \pm 9/2>+0.08 \pm 5/2>$
310.9	3.133	2.119	0.397	
470.2	0.304	1.021	2.820	
780.1	0.179	1.586	3.586	
1050.7	0.196	1.385	4.656	

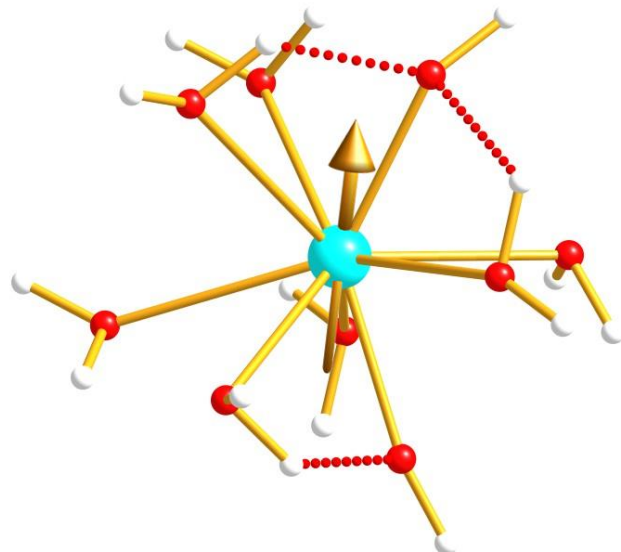


Figure S34: The g_{zz} axis of KD1 of pseudo capped square antiprismatic $[\text{U}(\text{OH})_3(\text{OH}_2)_6]$. It has been modelled from $[\text{U}(\text{H}_2\text{O})_9](\text{CF}_3\text{SO}_3)_3$.²⁴ Colour code: U-cyan, O-red and H-white.

Table S35: The computed energy of the five ground KDs of capped square antiprism $[\text{U}(\text{OH})_3(\text{OH}_2)_6]$ along with the g tensor and m_J composition of KD1.

Energy (cm^{-1})	g_x	g_y	g_z	m_J composition
0.0	0.480	0.968	4.860	$0.78 \pm 9/2> + 0.10 \pm 1/2> + 0.08 \pm 5/2>$
327.1	0.989	1.483	3.021	
684.3	1.155	1.396	2.908	
1026.1	2.831	1.950	0.498	
1260.7	0.163	0.429	4.103	

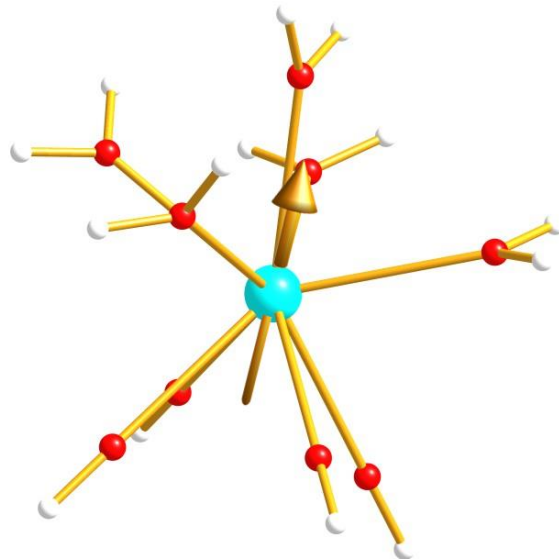


Figure S35: The g_{zz} axis of KD1 of pseudo tricapped trigonal prismatic $[\text{U}(\text{OH})_4(\text{OH}_2)_5]$. It has been modelled from $[\text{U}(\text{terpy})_3]\text{I}_3 \cdot 2\text{MeCN}$ (terpy = 2,2':6',2''-terpyridine).²³ Colour code: U-cyan, O-red and H-white.

Table S36: The computed energy of the five ground KDs of pseudo tricapped trigonal prismatic $[U(OH)_4(OH_2)_5]^-$ along with the g tensor and m_J composition of KD1.

Energy (cm ⁻¹)	g_x	g_y	g_z	m_J composition
0.0	0.993	1.271	4.128	$0.54 \pm 9/2 > + 0.15 \pm 1/2 > + 0.14 \pm 3/2 > + 0.09 \pm 7/2 >$
261.1	1.650	1.853	2.674	
438.4	0.370	0.930	2.788	
1014.4	0.672	1.352	3.176	
1407.2	0.305	1.787	3.748	

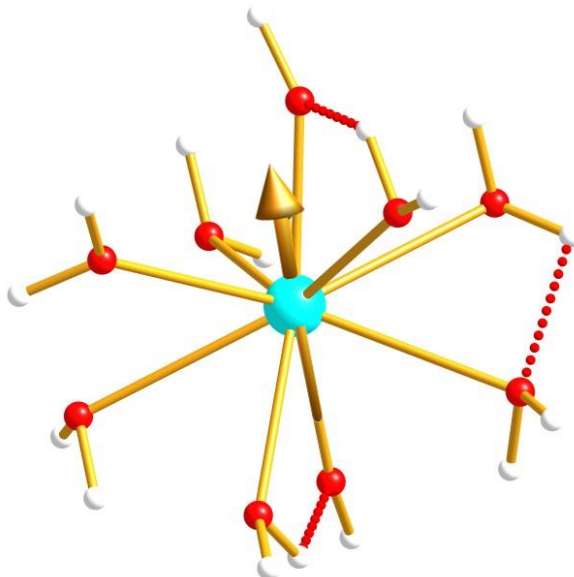


Figure S36: The g_{zz} axis of KD1 of pseudo tricapped trigonal prismatic $[U(OH)(OH_2)_8]^{2+}$. It has been modelled from $[U(\text{terpy})_3]\text{I}_3\cdot 2\text{MeCN}$ (terpy = 2,2':6',2''-terpyridine).²³ Colour code: U-cyan, O-red and H-white.

Table S37: The computed energy of the five ground KDs of pseudo tricapped trigonal prismatic $[U(OH)(OH_2)_8]^{2+}$ along with the g tensor and m_J composition of KD1.

Energy (cm ⁻¹)	g_x	g_y	g_z	m_J composition
0.0	0.344	0.371	5.246	$0.90 \pm 9/2 > + 0.06 \pm 3/2 >$
729.6	0.478	1.452	3.547	
1049.7	0.073	0.935	2.525	
1345.6	0.634	1.714	4.127	
1587.7	3.117	1.848	0.486	

Table S38: The computed energy of the five ground KDs of pseudo bicapped square antiprismatic $[U(OH)_2(OH_2)_8]^+$ along with the g tensor and m_J composition (see Figure S1 for the g_{zz} axis of KD1, it has been modelled from $[U(\text{OTf})_2(\text{phen})_4]^+$ (**22**, phen = 1,10-phenanthroline)).²²

Energy (cm ⁻¹)	g_x	g_y	g_z	m_J composition of the KDs
0.00	0.064	0.065	5.444	$0.99 \pm 7/2 >$
1128.3	0.298	0.307	3.134	$0.99 \pm 5/2 >$
1466.1	0.309	0.327	1.734	$0.99 \pm 3/2 >$

1819.9	3.250	3.231	0.399	$0.99\pm 1/2>$
2395.8	0.084	0.091	5.734	$0.99\pm 9/2>$

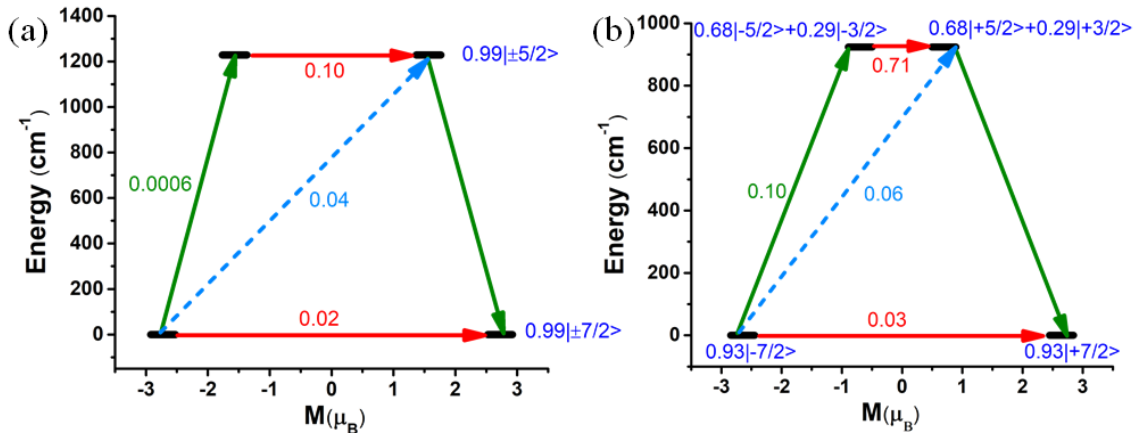


Figure S37: The mechanism of magnetic relaxation (a) pseudo bicapped square antiprismatic $[\text{U}(\text{OH})_2(\text{OH}_2)_8]^+$ (b) pseudo sphenocorona $[\text{U}(\text{OH})_3(\text{OH}_2)_7]$. See Figure S2 for colour description.

Table S39: The computed energy of the five ground KDs of pseudo sphenocorona $[\text{U}(\text{OH})_3(\text{OH}_2)_7]$ along with the g tensor and m_J composition (see Figure S1 for the g_{zz} axis of KD1).

Energy (cm^{-1})	g_x	g_y	g_z	m_J decomposition of the KDs
0.00	0.059	0.120	5.291	$0.93\pm 7/2>$
924.1	1.479	1.989	3.125	$0.68\pm 5/2>+0.29\pm 3/2>$
1116.4	3.059	1.742	0.018	$0.64\pm 3/2>+0.28\pm 5/2>$
1995.5	3.346	2.949	0.313	$0.93\pm 1/2>$
2460.0	0.162	0.373	5.516	$0.93\pm 9/2>$

Table S40: The computed energy of the five ground KDs of pseudo pentagonal antiprismatic $[\text{U}(\text{OH})_2(\text{OH}_2)_9]^+$ along with the g tensor and m_J composition (see Figure S1 for the g_{zz} axis of KD1, modelled from $[\text{U}(\text{H}_3\text{BNMe}_2\text{BH}_3)_3]$ (23)).²⁵

Energy (cm^{-1})	g_x	g_y	g_z	m_J composition of the KDs
0.00	0.016	0.125	5.420	$0.54\pm 7/2>+0.40\pm 9/2>$
898.0	1.537	1.878	3.161	$0.65\pm 5/2>+0.29\pm 3/2>$
1257.5	2.682	2.446	0.541	$0.55\pm 3/2>+0.30\pm 5/2>$
2083.4	0.789	1.316	3.719	$0.62\pm 1/2>+0.16\pm 7/2>+0.12\pm 9/2>$
2484.9	0.131	2.065	4.001	$0.43\pm 9/2>+0.24\pm 1/2>+0.24\pm 7/2>$

Table S41: The computed energy of the five ground KDs of pseudo pentagonal antiprismatic $[\text{U}(\text{OH})_3(\text{OH}_2)_8]$ along with the g tensor and m_J composition (see Figure S1 for the g_{zz} axis of KD1, modelled from $[\text{U}(\text{H}_3\text{BNMe}_2\text{BH}_3)_3]$ (23)).²⁵

Energy (cm^{-1})	g_x	g_y	g_z	m_J composition of the KDs
0.0	0.004	0.025	4.599	$0.62\pm 7/2>+0.17\pm 9/2>+0.14\pm 5/2>$
1564.5	0.469	0.750	2.678	$0.34\pm 5/2>+0.20\pm 1/2>+0.20\pm 3/2>$
2302.6	0.247	0.659	2.597	$0.49\pm 1/2>+0.23\pm 3/2>+0.18\pm 5/2>$

3331.2	0.009	1.069	3.961	$0.36 9/2>+0.24 7/2>+0.17 3/2>$
4106.1	0.163	0.774	3.070	$0.38 3/2>+0.22 9/2>+0.15 1/2>$

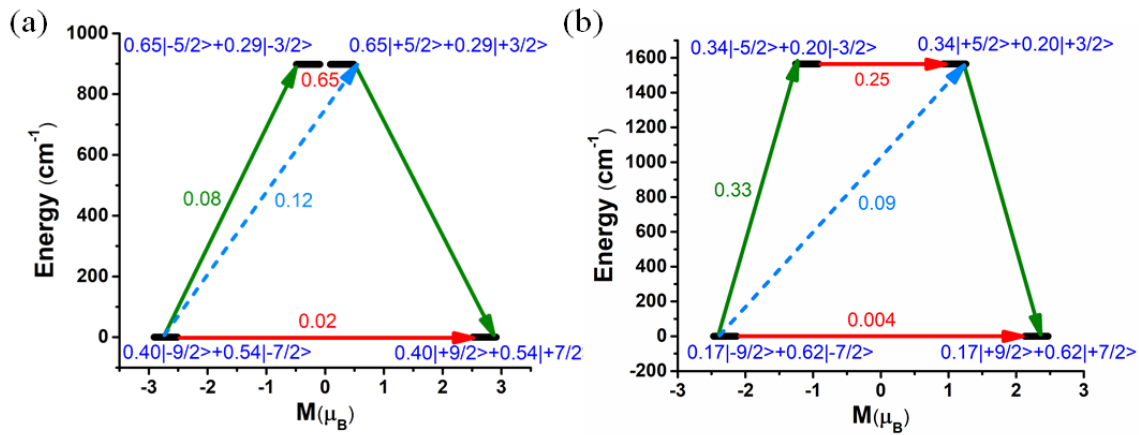


Figure S38: The mechanism of magnetic relaxation pseudo pentagonal antiprismatic (a) $[\text{U}(\text{OH})_2(\text{OH}_2)_9]^+$ (b) $[\text{U}(\text{OH})_3(\text{OH}_2)_8]$. See Figure S2 for colour description.

Table S42: The computed energy of the five ground KDs of pseudo icosahedron $[\text{U}(\text{OH})_2(\text{OH}_2)_{10}]^+$ along with the g tensor and m_J composition (see Figure S1 for the g_{zz} axis of KD1, modelled from $[\text{U}(\text{H}_3\text{BNMe}_2\text{BH}_3)_3]$ (23)).²⁵

Energy (cm^{-1})	g_x	g_y	g_z	m_J composition of the KDs
0.00	0.042	0.203	5.036	$0.72 9/2>+0.20 7/2>$
820.6	0.930	1.464	3.051	$0.54 5/2>+0.37 3/2>$
1054.1	0.646	1.357	3.048	$0.52 3/2>+0.40 5/2>$
1919.6	3.836	2.522	0.399	$0.90 1/2>$
2374.0	0.055	0.616	4.644	$0.70 7/2>+0.18 9/2>$

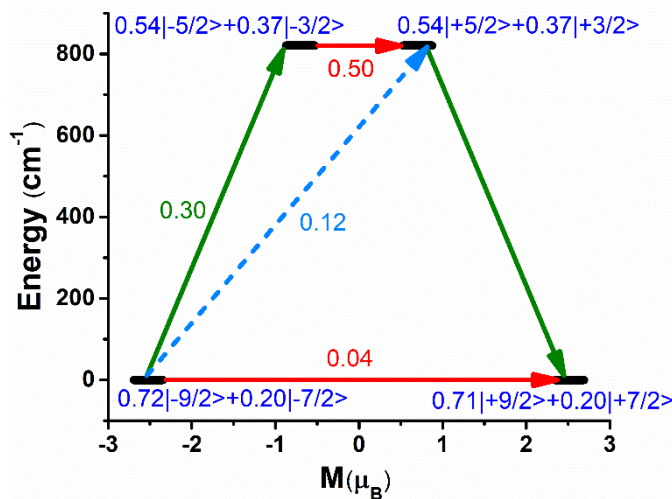


Figure S39: The mechanism of magnetic relaxation pseudo icosahedron $[\text{U}(\text{OH})_2(\text{OH}_2)_{10}]^+$. See Figure S2 for colour description.

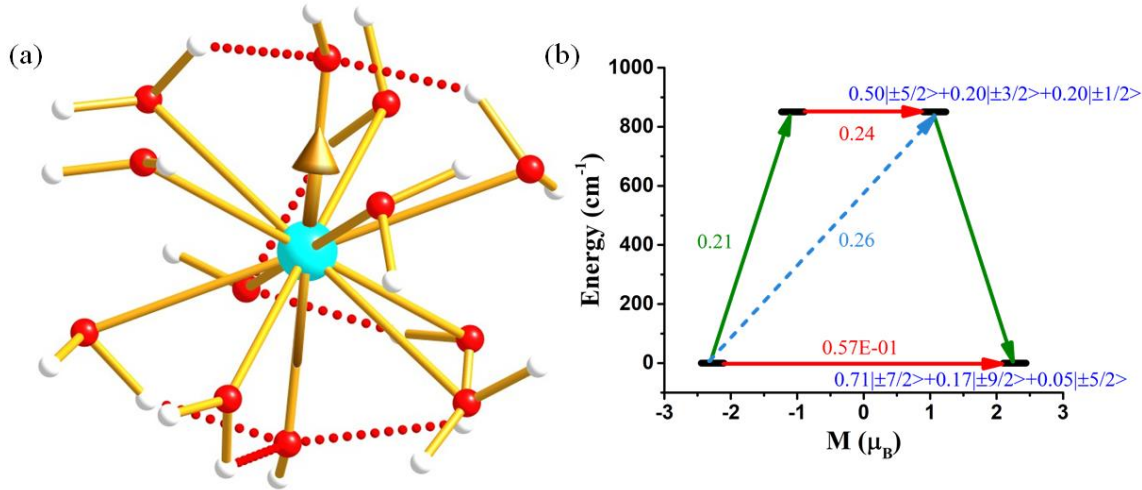


Table S43: The computed energy of the five ground KDs of pseudo icosahedron $[\text{U}(\text{OH})_3(\text{OH}_2)_9]$ along with the g tensor and m_J composition.

Energy (cm ⁻¹)	g_x	g_y	g_z
0.0	0.002	0.340	4.546
850.6	0.446	0.746	3.220
1119.7	0.120	0.258	2.817
2153.3	0.503	1.506	3.415
2625.2	0.532	0.641	4.409

Table S44: The computed energy of the five ground KDs of **1** along with the g tensor.

Energy (cm ⁻¹)	g_x	g_y	g_z
0.0	0.151	0.182	5.741
962.3	0.386	0.601	4.368
1386.8	0.252	1.353	4.664
1920.7	3.271	1.911	0.238
2257.7	3.257	3.223	1.092

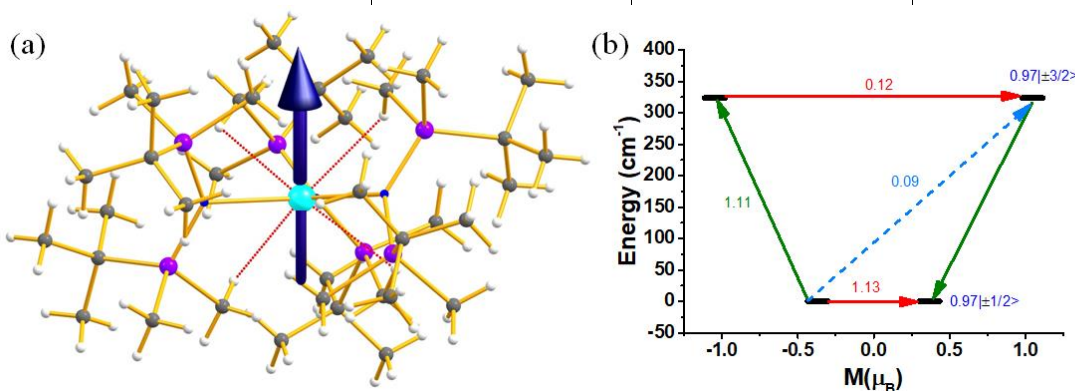


Figure S41: (a) The g_{zz} axis of KD1 of **2**. Colour code: U-cyan, Si-purple, N-blue, C-grey and H-white. (b) The mechanism of magnetic relaxation of **2**. See Figure S2 for colour description.

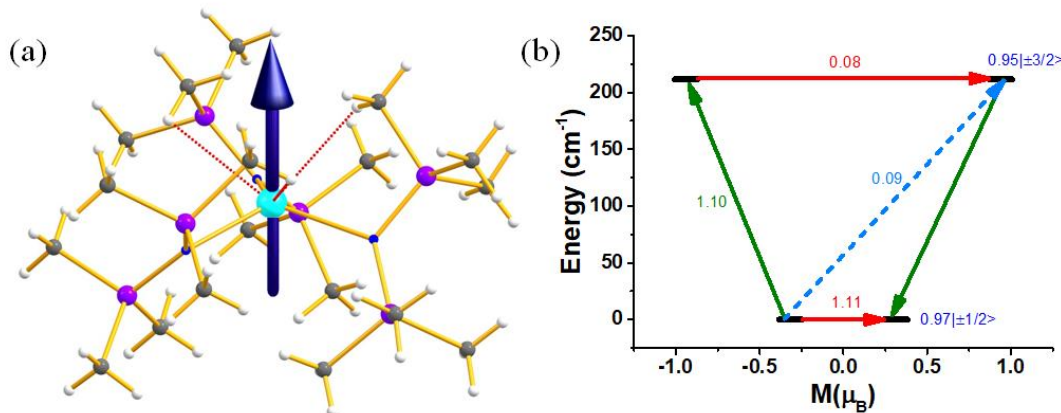


Figure S42: (a) The g_{zz} axis of KD1 of 3. Colour code: U-cyan, Si-purple, N-blue, C-grey and H-white. (b) The mechanism of magnetic relaxation of 3. See Figure S2 for colour description.

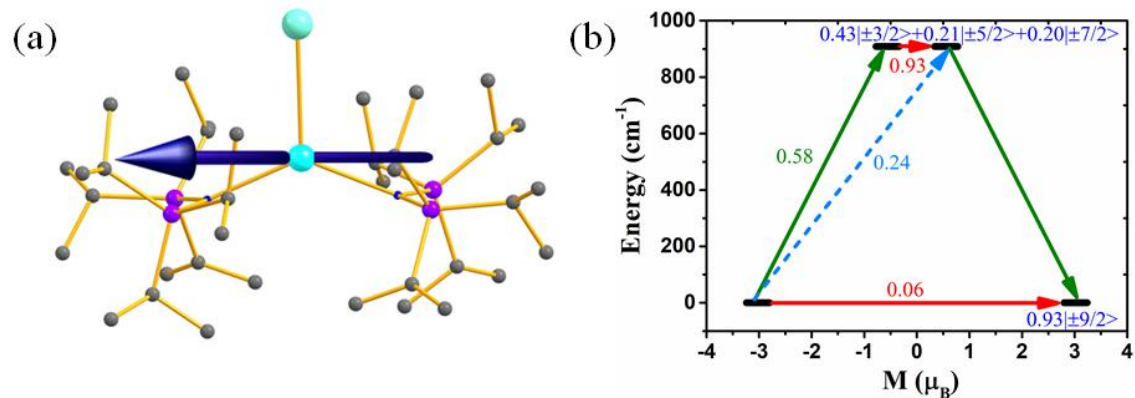


Figure S43: (a) The g_{zz} axis of KD1 of 4. Colour code: U-cyan, Si-purple, N-blue and C-grey. Hydrogens are omitted for clarity. (b) The mechanism of magnetic relaxation of 4. See Figure S2 for colour description.

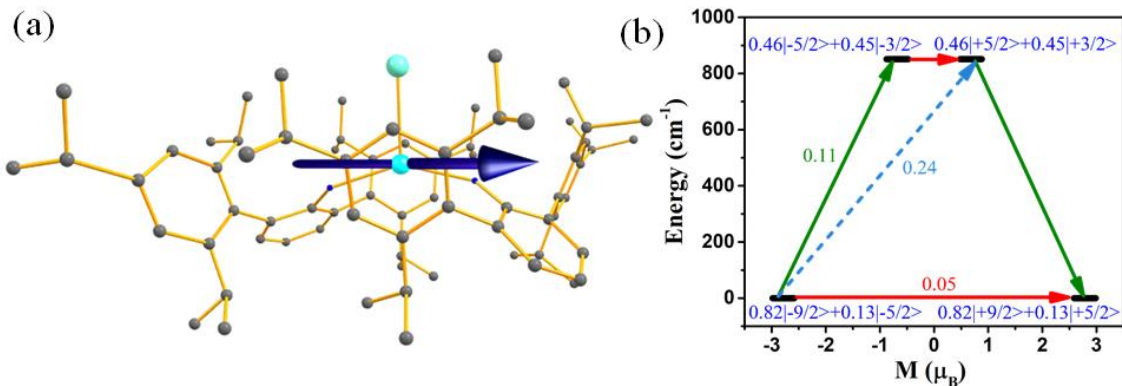


Figure S44: (a) The g_{zz} axis of KD1 of 5. Colour code: U-cyan, Si-purple, N-blue and C-grey. Hydrogens are omitted for clarity. (b) The mechanism of magnetic relaxation of 5. See Figure S2 for colour description.

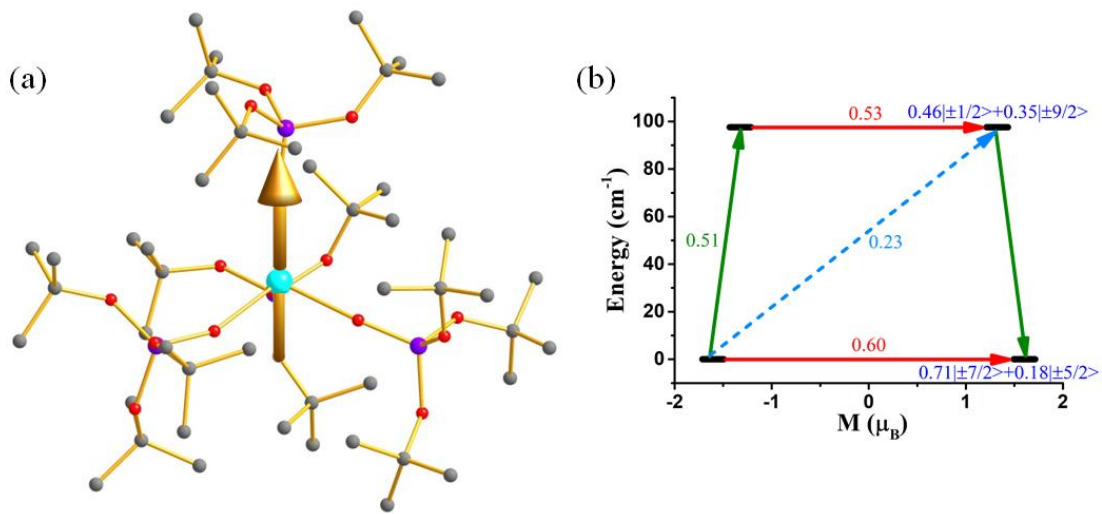


Figure S45: (a) The g_{zz} axis of KD1 of **6**. Colour code: U-cyan, Si-purple, O-red and C-grey. Hydrogens are omitted for clarity. (b) The mechanism of magnetic relaxation of **6**. See Figure S2 for colour description.

Table S45: The computed energy of the five ground KDs of **6** along with the g tensor and m_J composition.

Energy (cm^{-1})	g_x	g_y	g_z
0.0	1.639	1.960	3.207
97.6	2.833	2.157	0.328
169.9	0.268	1.496	3.519
1065.5	0.577	1.510	3.825
1082.0	0.271	1.780	3.657

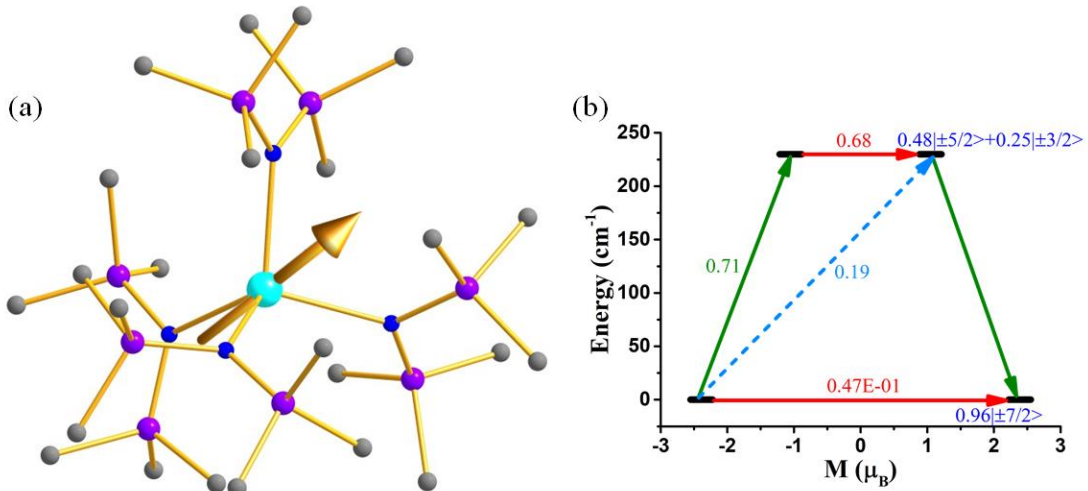


Figure S46: (a) The g_{zz} axis of KD1 of **7**. Colour code: U-cyan, Si-purple, N-blue and C-grey. Hydrogens are omitted for clarity. (b) The mechanism of magnetic relaxation of **7**. See Figure S1 for colour description.

Table S46: The computed energy of the five ground KDs of **7** along with the g tensor.

Energy (cm ⁻¹)	g_x	g_y	g_z
0.0	0.040	0.243	4.774
229.8	2.858	2.033	1.145
253.7	0.435	1.722	3.231
589.2	1.753	2.158	3.170
687.1	3.732	2.659	0.183

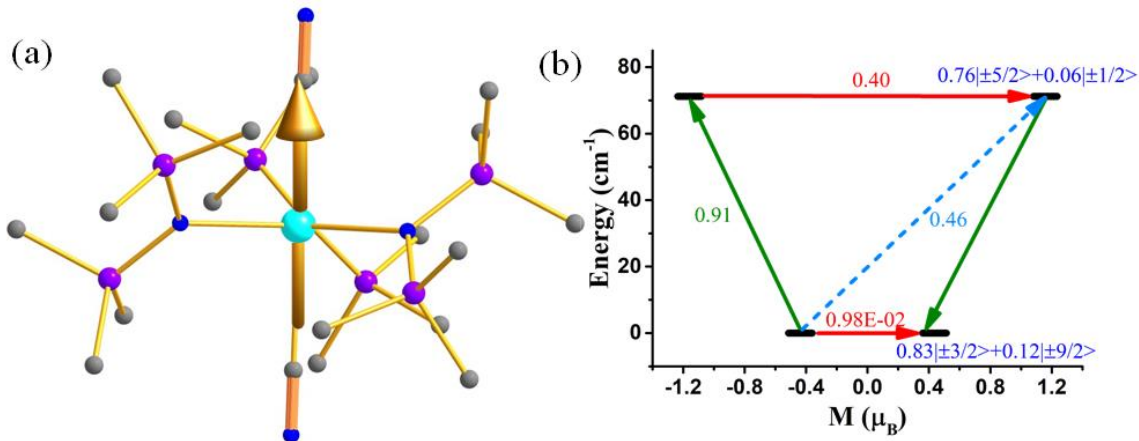


Figure S47: (a) The g_{zz} axis of KD1 of **8**. Colour code: U-cyan, Si-purple, N-blue and C-grey. Hydrogens are omitted for clarity. (b) The mechanism of magnetic relaxation of **8**. See Figure S2 for colour description.

Table S47: The computed energy of the five ground KDs of **8** along with the g tensor and m_J composition.

Energy (cm ⁻¹)	g_x	g_y	g_z
0.0	0.022	0.037	0.873
71.2	1.153	1.242	2.321
320.4	3.115	3.083	0.613
529.0	0.007	0.010	4.981
1261.6	1.752	1.756	3.894

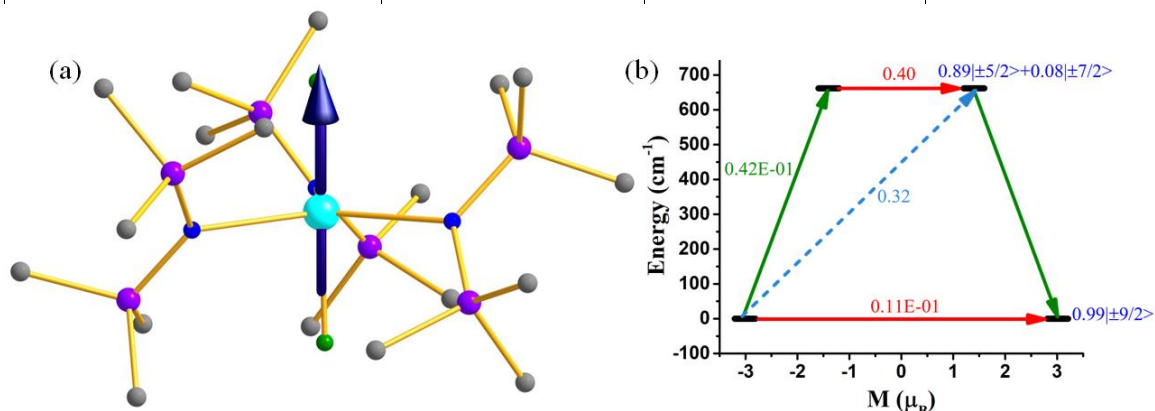


Figure S48: (a) The g_{zz} axis of KD1 of **8F**. Colour code: U-cyan, Si-purple, N-blue and C-grey. Hydrogens are omitted for clarity. (b) The mechanism of magnetic relaxation of **8F**. See Figure S2 for colour description.

Table S48: The computed energy of the five ground KDs of **8F** along with the g tensor and m_J composition of five KDs (using MOLCAS 8.2).

Energy (cm ⁻¹)	g_x	g_y	g_z	m_J composition (using “CRYST” = U)	m_J composition (using “CRYST” = Nd)
0.0	0.032	0.034	6.020	0.99 ±9/2>	0.99 ±9/2>
661.8	0.669	1.664	2.863	0.88 ±5/2>+0.07 ±7/2>	0.88 ±5/2>+0.07 ±7/2>
726.6	1.798	1.216	0.249	0.97 ±3/2>	0.97 ±3/2>
961.5	3.834	2.566	0.808	0.91 ±1/2>+0.07 ±3/2>	0.91 ±1/2>+0.07 ±3/2>
1375.8	1.595	1.688	4.206	0.86 ±7/2>+0.09 ±5/2>	0.86 ±7/2>+0.09 ±5/2>

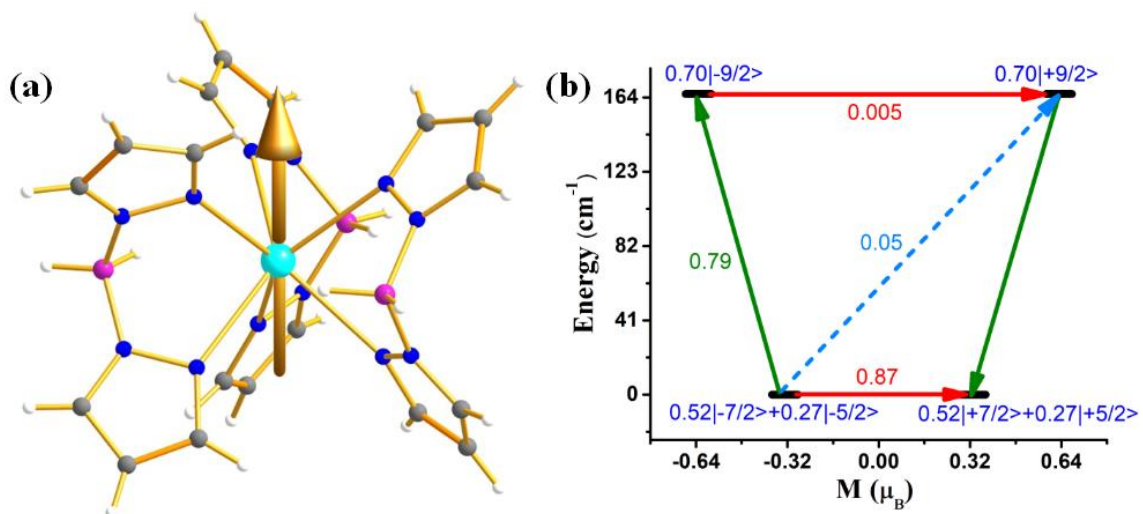


Figure S49: (a) The g_{zz} axis of KD1 of **9**. Colour code: U-cyan, Si-purple, N-blue, C-grey and H-white.
(b) The mechanism of magnetic relaxation of **9**. See Figure S2 for colour description.

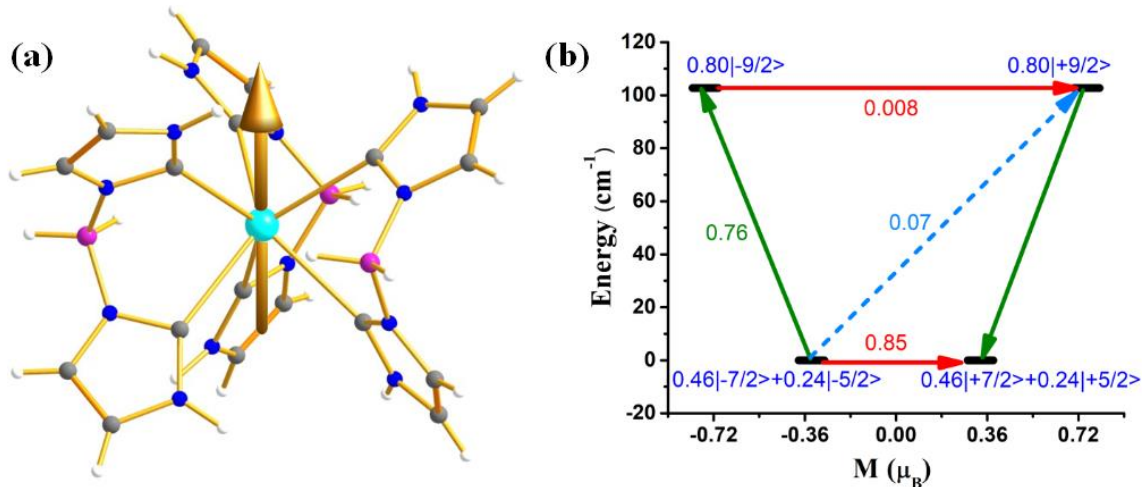


Figure S50: (a) The g_{zz} axis of KD1 of **10**. Colour code: U-cyan, Si-purple, N-blue, C-grey and H-white.
(b) The mechanism of magnetic relaxation of **10**. See Figure S2 for colour description.

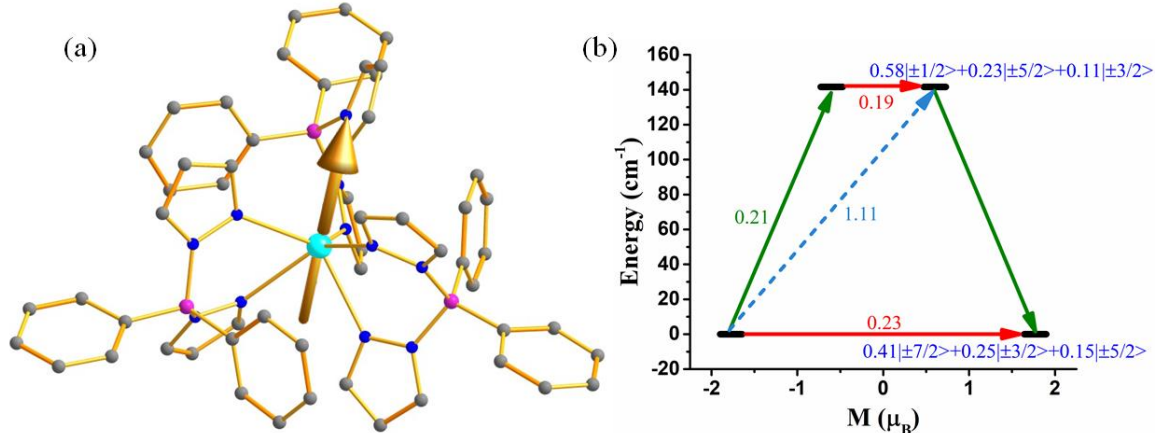


Table S49: The computed energy of the five ground KDs of **11** along with the g tensor.

Energy (cm ⁻¹)	g_x	g_y	g_z
0.0	0.283	1.115	3.542
141.7	0.334	0.575	2.204
389.3	0.477	1.190	4.706
449.2	0.715	1.844	3.308
477.8	3.503	2.054	0.348

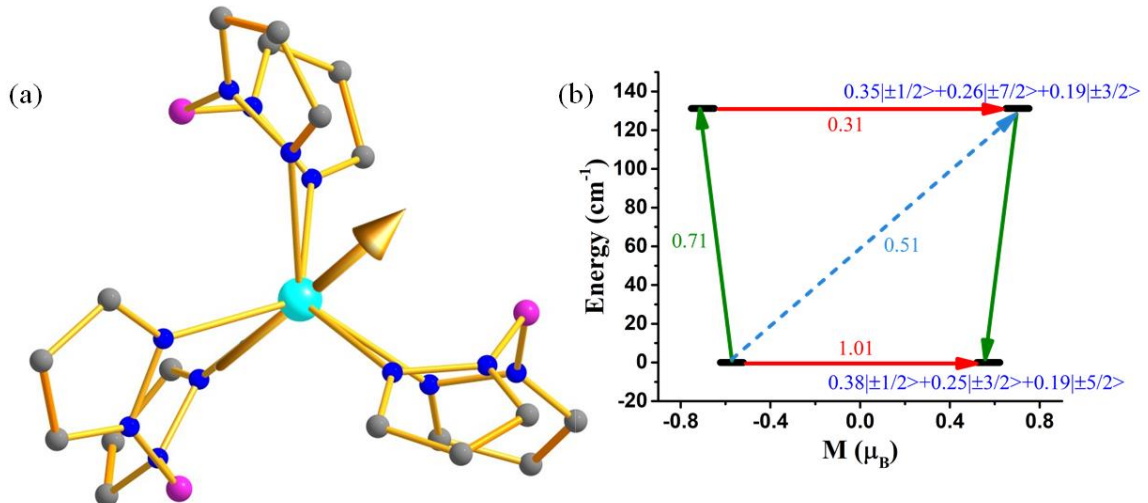


Table S50: The computed energy of the five ground KDs of **12** along with the g tensor.

Energy (cm ⁻¹)	g_x	g_y	g_z
0.0	3.482	2.591	1.143
131.3	0.478	1.071	4.552
288.8	2.779	1.844	0.103

389.8	2.350	1.427	0.453
472.9	0.236	0.789	4.104

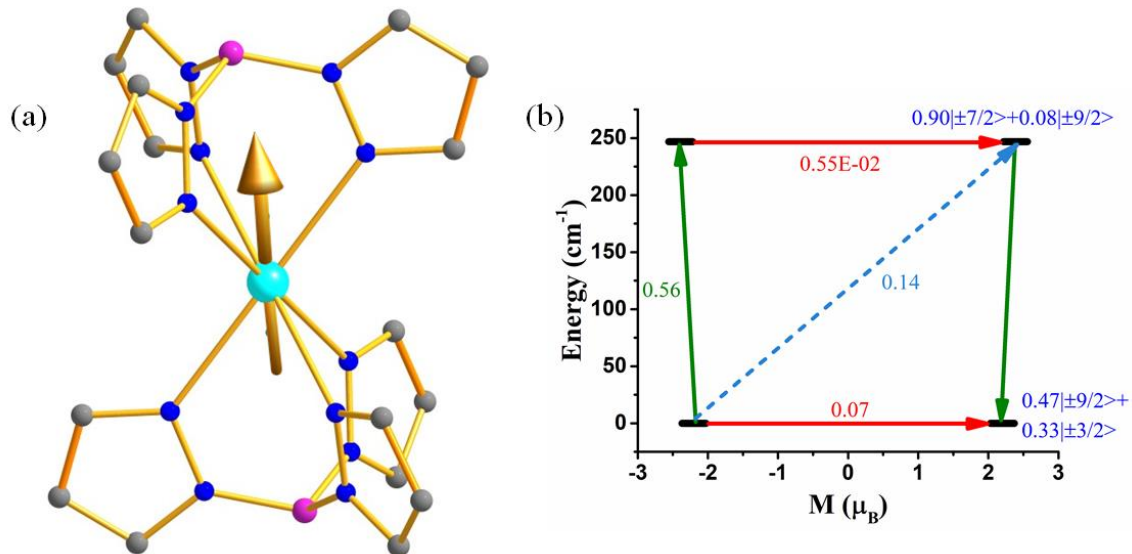


Figure S53: (a) The g_{zz} axis of KD1 of **13**. Colour code: U-cyan, B-pink, N-blue and C-grey. Hydrogens are omitted for clarity. (b) The mechanism of magnetic relaxation of **13**. See Figure S2 for colour description.

Table S51: The computed energy of the five ground KDs of **13** along with the g tensor.

Energy (cm^{-1})	g_x	g_y	g_z
0.0	0.085	0.345	4.398
246.9	0.010	0.021	4.981
518.3	0.024	0.983	3.648
1343.6	3.053	2.716	0.114
1801.3	0.379	0.546	4.161

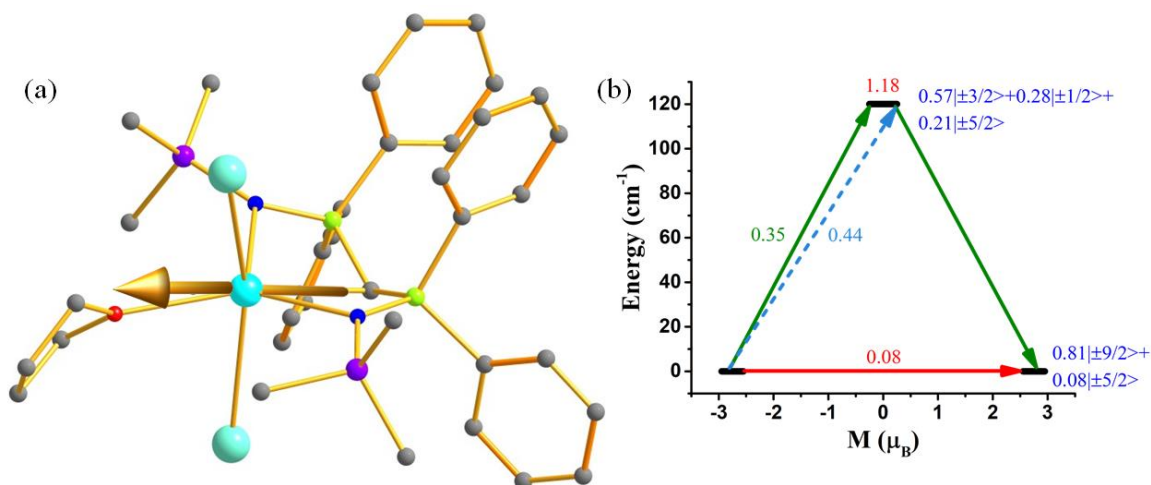


Figure S54: (a) The g_{zz} axis of KD1 of **14**. Colour code: U-cyan, I-aqua, P-lime, Si-purple, O-red, N-blue and C-grey. Hydrogens are omitted for clarity. (b) The mechanism of magnetic relaxation of **14**. See Figure S2 for colour description.

Table S52: The computed energy of the five ground KDs of **14** along with the g tensor.

Energy (cm ⁻¹)	g _x	g _y	g _z
0.0	0.174	0.316	5.500
120.1	0.027	0.183	5.518
325.3	1.741	2.079	3.585
484.7	0.317	0.853	5.307
555.1	0.257	1.193	4.638

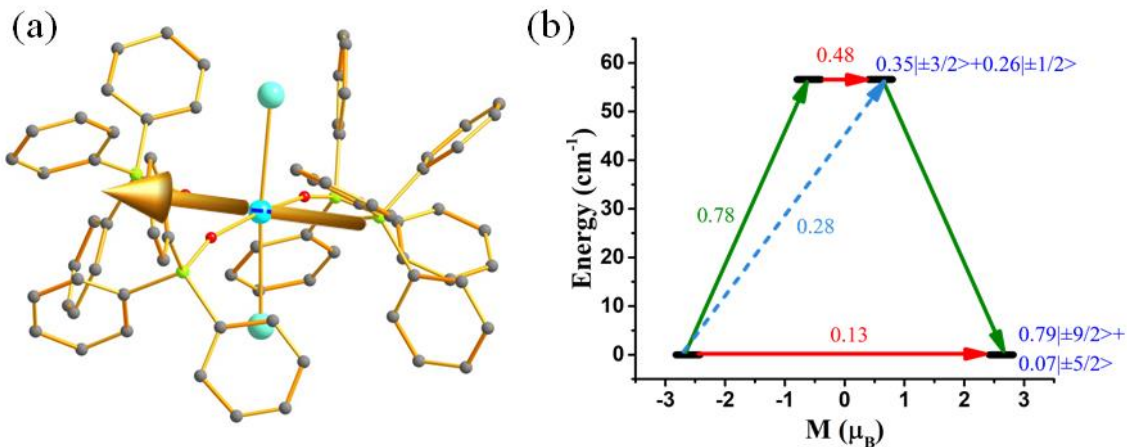


Figure S55: The g_{zz} axis of KD1 of **15**. Colour code: U-cyan, I-aqua, P-lime, N-blue and C-grey. Hydrogens are omitted for clarity. The mechanism of magnetic relaxation (b) **15**. See Figure S2 for colour description.

Table S53: The computed energy of the five ground KDs of **15** along with the g tensor.

Energy (cm ⁻¹)	g _x	g _y	g _z
0.0	0.151	0.620	5.241
56.6	0.030	0.521	5.105
542.6	0.608	0.681	5.922
817.6	0.304	0.765	4.717
877.0	1.694	2.471	3.509

Table S54: The computed energy of the five ground KDs of **15F** along with the g tensor.

Energy (cm ⁻¹)	g _x	g _y	g _z
0.0	0.022	0.024	5.727
725.2	2.810	2.449	0.535
1337.2	3.217	2.777	0.573
1772.6	2.966	2.869	1.301
2169.2	0.301	0.525	4.292

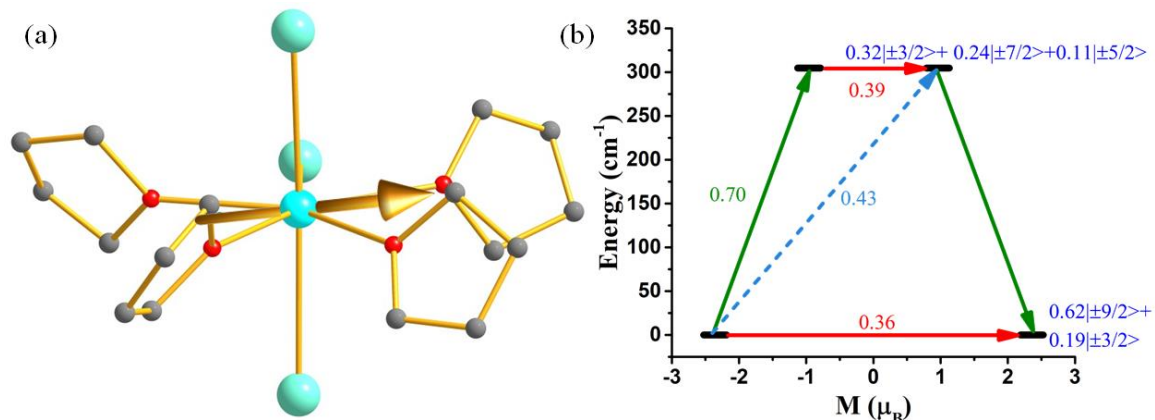


Figure S56: (a) The g_{zz} axis of KD1 of **16**. Colour code: U-cyan, Si-purple, N-blue and C-grey. Hydrogens are omitted for clarity. (b) The mechanism of magnetic relaxation of **16**. See Figure S2 for colour description.

Table S55: The computed energy of the five ground KDs of **16** along with the g tensor.

Energy (cm^{-1})	g_x	g_y	g_z
0.0	0.491	1.690	4.712
304.8	0.708	1.435	2.466
539.4	0.681	2.167	3.680
576.4	0.413	1.379	2.751
734.5	3.169	2.585	0.668

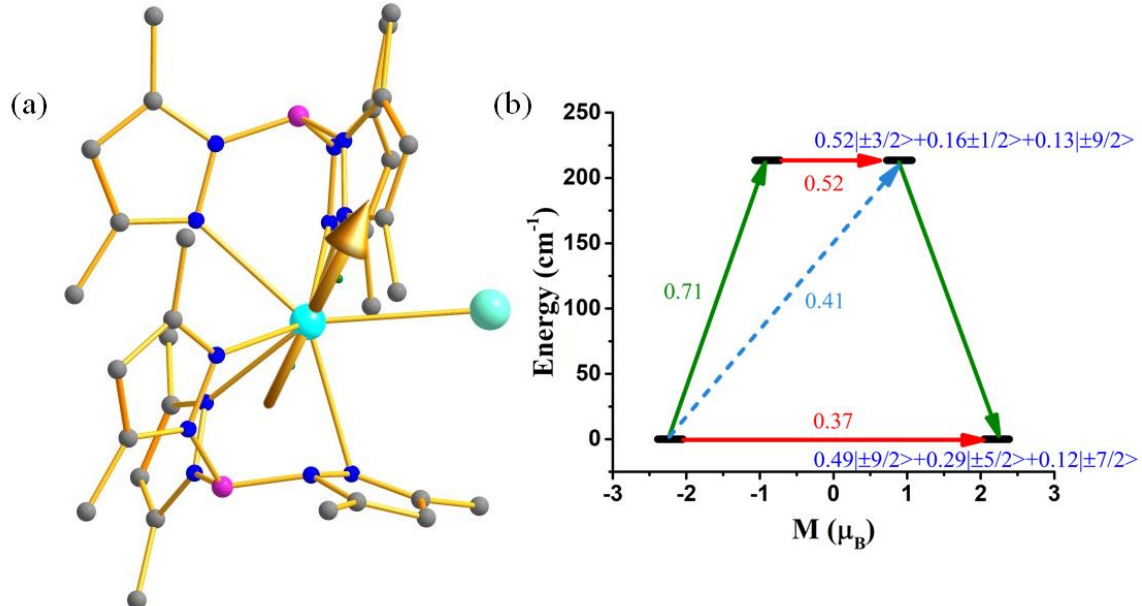


Figure S57: (a) The g_{zz} axis of KD1 of **17**. Colour code: U-cyan, I-aqua, N-blue and C-grey. Hydrogens are omitted for clarity. (b) The mechanism of magnetic relaxation of **17**. See Figure S2 for colour description.

Table S56: The computed energy of the five ground KDs of **17** along with the g tensor.

Energy (cm ⁻¹)	g_x	g_y	g_z
0.0	0.700	1.503	4.434
213.6	3.274	2.130	0.266
423.1	0.250	1.207	4.099
620.4	0.162	0.508	3.894
793.5	1.367	1.898	4.024

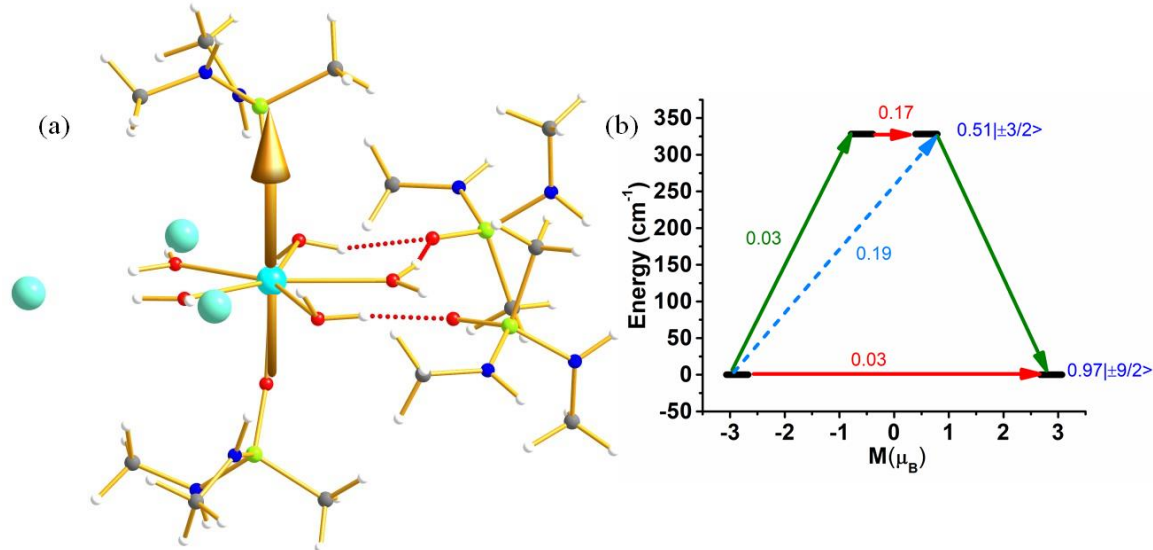


Figure S58: (a) The g_{zz} axis of KD1 of **18**. Colour code: U-cyan, I-aqua, P-lime, O-red, N-blue, C-grey and H-white. (b) The mechanism of magnetic relaxation of **18**. See Figure S2 for colour description.

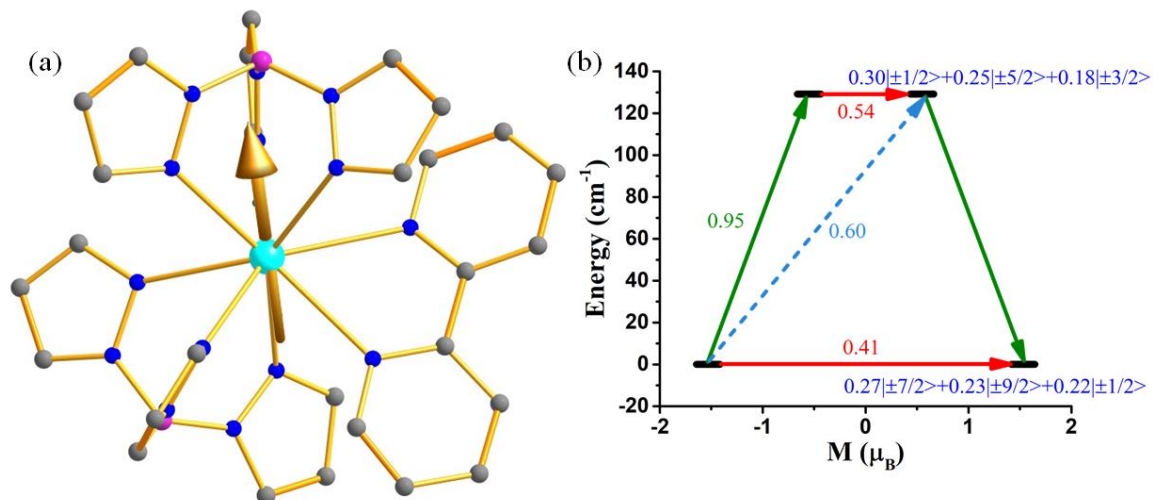


Figure S59: (a) The g_{zz} axis of KD1 of $[U(Tp^{Me^2})_2(bipy)]^+$ (**19**). Colour code: U-cyan, I-aqua, P-lime, O-red, N-blue, C-grey and H-white. (b) The mechanism of magnetic relaxation of **19**. See Figure S2 for colour description.

Table S57: The computed energy of the five ground KDs of **19** along with the g tensor.

Energy (cm ⁻¹)	g _x	g _y	g _z
0.0	0.656	1.797	3.061
129.2	0.644	1.027	2.765
400.8	2.731	2.151	0.339
556.7	2.817	1.830	0.230
789.3	0.185	0.954	4.509

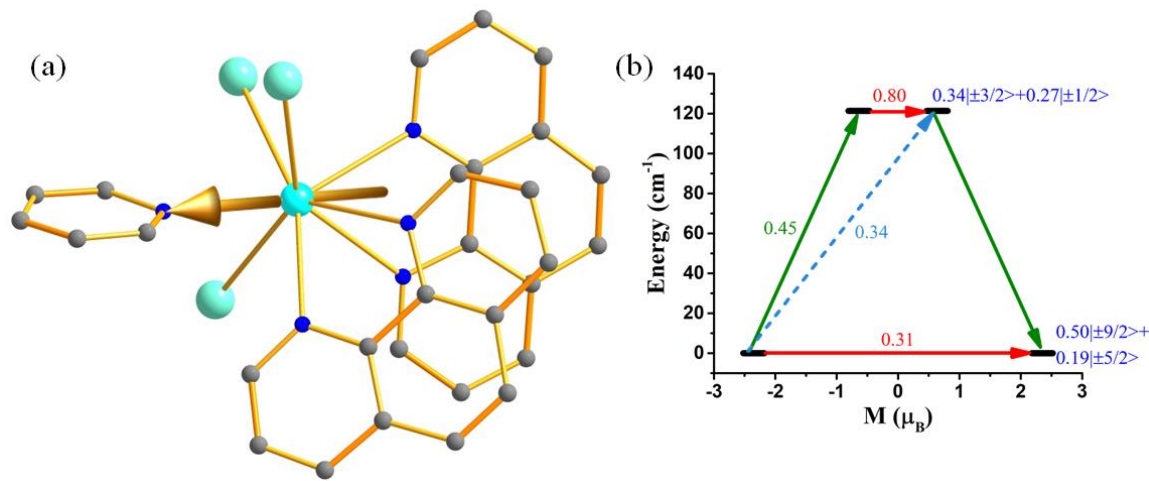


Figure S60: (a) The g_{zz} axis of KD1 of [UI₃(Me₄phen)₂(py)] (21). Colour code: U-cyan, I-aqua, P-lime, N-blue, C-grey. Hydrogens are omitted for clarity. (b) The mechanism of magnetic relaxation of **21**. See Figure S2 for colour description.

Table S58: The computed energy of the five ground KDs of **21** along with the g tensor.

Energy (cm ⁻¹)	g _x	g _y	g _z
0.0	0.771	1.104	4.699
121.4	0.939	1.764	3.776
271.3	0.172	1.815	3.625
612.3	0.219	1.066	3.483
863.9	0.710	1.628	3.899

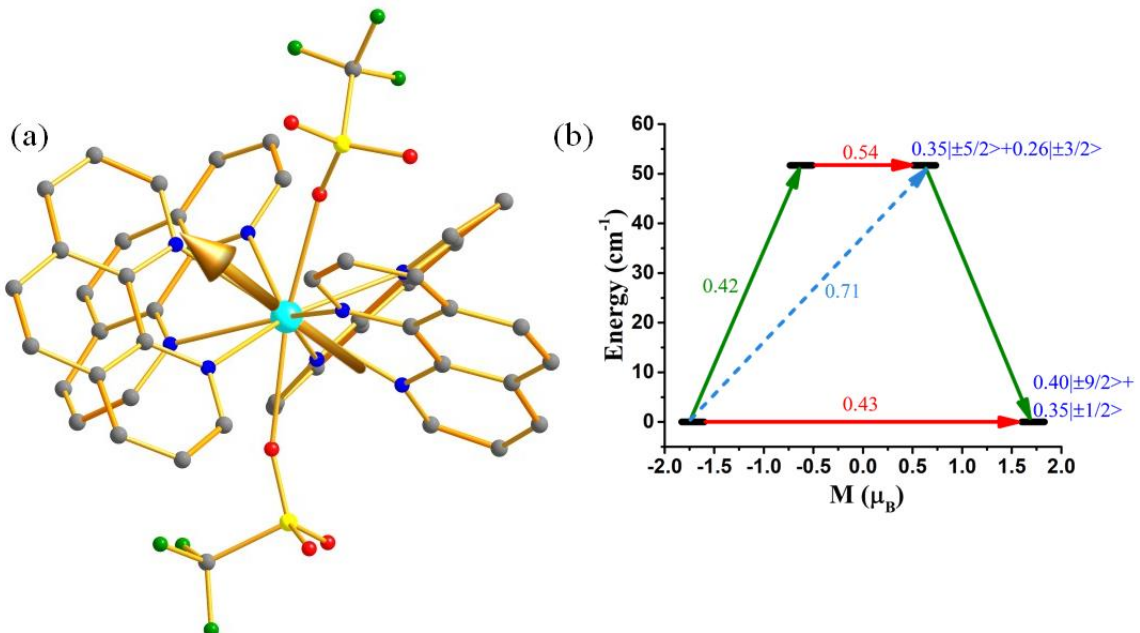
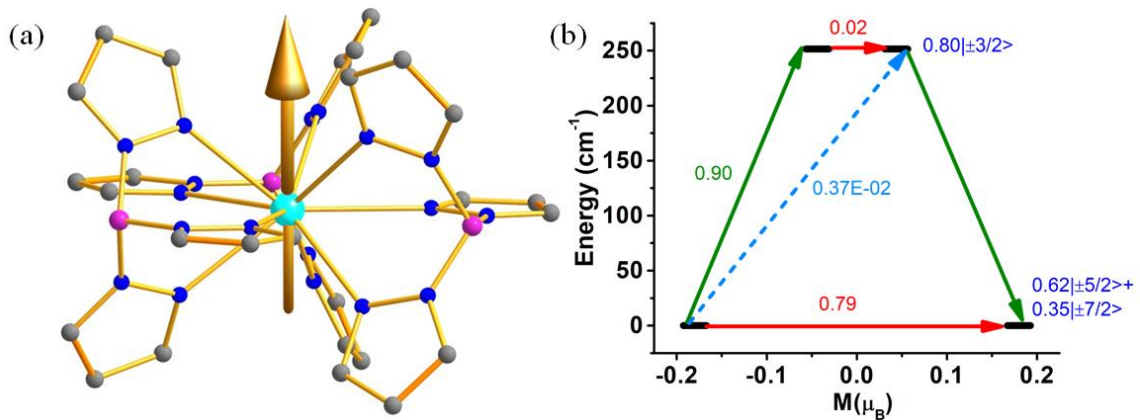


Table S59: The computed energy of the five ground KDs of **23** along with the g tensor.

Energy (cm ⁻¹)	g_x	g_y	g_z
0.0	1.016	1.549	3.430
51.7	2.018	1.632	0.905
183.9	0.387	1.107	3.252
552.2	0.040	1.582	3.276
950.1	0.998	2.053	4.062

Appendix S1: The optimised cartesian coordinates of **1**.

U	-0.010540000	0.011357000	0.346779000
N	2.243768000	-0.624999000	-0.126996000
C	2.876840000	-1.798866000	-0.533596000
C	2.080106000	-2.975038000	-0.583380000
C	0.681331000	-2.837288000	-0.078730000
C	-0.415606000	-2.694620000	-0.975945000
C	-0.217460000	-2.795455000	-2.487866000
H	0.849563000	-2.610483000	-2.683559000
C	-0.539087000	-4.222067000	-2.979404000
H	0.047504000	-4.984575000	-2.450527000
H	-0.318647000	-4.312901000	-4.054283000
H	-1.606380000	-4.454069000	-2.832928000
C	-1.025143000	-1.767921000	-3.296088000
H	-2.097243000	-2.008124000	-3.320453000
H	-0.674042000	-1.754545000	-4.338678000
H	-0.929586000	-0.742771000	-2.902699000
C	-1.711106000	-2.517062000	-0.446676000
H	-2.557327000	-2.447345000	-1.132225000
C	-1.961587000	-2.479815000	0.935495000
C	-3.388130000	-2.496802000	1.468509000
H	-4.008084000	-1.880795000	0.794341000
C	-3.530207000	-1.943149000	2.890744000
H	-3.045379000	-2.594295000	3.635316000
H	-4.591953000	-1.881641000	3.165969000
H	-3.102703000	-0.932706000	2.987592000
C	-3.941108000	-3.937057000	1.394081000
H	-3.858810000	-4.354160000	0.379163000
H	-5.004030000	-3.950972000	1.679958000
H	-3.395106000	-4.605288000	2.079165000
C	-0.852393000	-2.552121000	1.797388000
H	-1.023124000	-2.521692000	2.872711000
C	0.458000000	-2.755591000	1.327385000
C	1.598022000	-2.976119000	2.319001000
H	2.521528000	-2.632755000	1.832059000
C	1.759515000	-4.482177000	2.616730000
H	0.899963000	-4.862683000	3.191994000
H	2.668887000	-4.655751000	3.212406000
H	1.844631000	-5.074989000	1.696163000
C	1.459063000	-2.187102000	3.629242000
H	1.302203000	-1.108083000	3.455559000
H	2.380167000	-2.287036000	4.222021000
H	0.633307000	-2.551673000	4.260099000
C	2.604998000	-4.187657000	-1.039044000
H	1.972646000	-5.077966000	-1.057262000
C	3.931707000	-4.265866000	-1.464555000
H	4.342910000	-5.207071000	-1.833572000

C	4.737563000	-3.129340000	-1.365433000
H	5.794542000	-3.199689000	-1.631737000
C	4.256554000	-1.903053000	-0.879437000
C	5.254658000	-0.804405000	-0.621257000
C	5.585701000	0.153117000	-1.615114000
C	4.906183000	0.159982000	-2.985541000
H	3.920161000	-0.317220000	-2.863420000
C	4.682083000	1.573077000	-3.548909000
H	4.191143000	2.236721000	-2.820909000
H	4.055498000	1.530304000	-4.453353000
H	5.628463000	2.054328000	-3.839894000
C	5.699374000	-0.681520000	-4.005757000
H	6.719040000	-0.283399000	-4.131757000
H	5.206516000	-0.665233000	-4.991186000
H	5.786303000	-1.731048000	-3.691376000
C	6.607015000	1.077992000	-1.352752000
H	6.869638000	1.811245000	-2.118688000
C	7.321569000	1.093841000	-0.149362000
C	6.993628000	0.127521000	0.808686000
H	7.563938000	0.088059000	1.738627000
C	5.991026000	-0.829319000	0.595186000
C	5.829497000	-1.967633000	1.607949000
H	4.887875000	-2.485229000	1.374851000
C	6.962909000	-2.998492000	1.436247000
H	6.992528000	-3.399198000	0.412436000
H	6.828480000	-3.846218000	2.127605000
H	7.945612000	-2.546344000	1.646072000
C	5.739494000	-1.505086000	3.069071000
H	6.648505000	-0.979254000	3.400765000
H	5.611859000	-2.372691000	3.736047000
H	4.886304000	-0.830365000	3.227118000
C	8.467884000	2.080001000	0.044700000
H	8.292489000	2.907783000	-0.664368000
C	8.529640000	2.690095000	1.452313000
H	7.578625000	3.173462000	1.727614000
H	9.322018000	3.452675000	1.505134000
H	8.758772000	1.934147000	2.220272000
C	9.813177000	1.430545000	-0.334960000
H	10.035921000	0.573811000	0.321779000
H	10.639068000	2.153496000	-0.239667000
H	9.801669000	1.061254000	-1.371733000
N	-2.273098000	0.650354000	-0.089907000
C	-2.901102000	1.829952000	-0.487949000
C	-2.090840000	2.994921000	-0.514955000
C	-2.596870000	4.221574000	-0.953567000
H	-1.953333000	5.104298000	-0.950976000
C	-3.922992000	4.322633000	-1.377635000
H	-4.321356000	5.274227000	-1.733839000

C	-4.741881000	3.192406000	-1.305931000
H	-5.795825000	3.277696000	-1.579927000
C	-4.275491000	1.950428000	-0.844388000
C	-5.283065000	0.851025000	-0.627985000
C	-5.637892000	-0.047981000	-1.665810000
C	-6.674081000	-0.968684000	-1.444911000
H	-6.953877000	-1.656836000	-2.245930000
C	-7.379551000	-1.033417000	-0.239404000
C	-8.513401000	-2.033389000	-0.051779000
H	-8.588927000	-2.605815000	-0.992079000
C	-9.867136000	-1.334183000	0.165152000
H	-9.869295000	-0.734878000	1.089782000
H	-10.677922000	-2.075181000	0.249520000
H	-10.108656000	-0.660297000	-0.671111000
C	-8.221028000	-3.039707000	1.074761000
H	-7.263343000	-3.559200000	0.911687000
H	-9.013085000	-3.803110000	1.131137000
H	-8.171953000	-2.541622000	2.057031000
C	-7.026371000	-0.124174000	0.765685000
H	-7.584164000	-0.130305000	1.705065000
C	-6.008742000	0.823826000	0.595076000
C	-5.811557000	1.890691000	1.675136000
H	-4.877948000	2.425244000	1.448690000
C	-5.676057000	1.318714000	3.093278000
H	-6.599998000	0.824989000	3.433581000
H	-5.459943000	2.124680000	3.812868000
H	-4.861166000	0.583888000	3.153146000
C	-6.945439000	2.933058000	1.617513000
H	-7.014296000	3.398361000	0.622909000
H	-6.777133000	3.734667000	2.355048000
H	-7.921595000	2.472870000	1.839266000
C	-4.970154000	0.001115000	-3.040344000
H	-3.993108000	0.494820000	-2.913890000
C	-4.721980000	-1.391965000	-3.643460000
H	-4.214812000	-2.064663000	-2.934761000
H	-4.101011000	-1.313605000	-4.549550000
H	-5.660602000	-1.883536000	-3.942184000
C	-5.788679000	0.854152000	-4.029827000
H	-6.787617000	0.417539000	-4.189643000
H	-5.283755000	0.908331000	-5.007873000
H	-5.927819000	1.882195000	-3.666570000
C	-0.437300000	2.742509000	1.375895000
C	0.880202000	2.518499000	1.818354000
H	1.072367000	2.494900000	2.890363000
C	1.968231000	2.418931000	0.931033000
C	3.412558000	2.406892000	1.416595000
H	3.969980000	1.684997000	0.794393000
C	4.045374000	3.793795000	1.170696000

H	3.980183000	4.094019000	0.114251000
H	5.109445000	3.779318000	1.450870000
H	3.544017000	4.567641000	1.773905000
C	3.578222000	2.000897000	2.884117000
H	3.162126000	2.757560000	3.568264000
H	4.645219000	1.900108000	3.126536000
H	3.096122000	1.036241000	3.106669000
C	1.684646000	2.448169000	-0.444461000
H	2.512846000	2.356231000	-1.149794000
C	0.382363000	2.649094000	-0.944458000
C	0.149381000	2.740266000	-2.451513000
H	-0.930121000	2.607214000	-2.616256000
C	0.527458000	4.142734000	-2.969836000
H	-0.051389000	4.935600000	-2.476953000
H	0.338409000	4.210742000	-4.052322000
H	1.596653000	4.349190000	-2.801009000
C	0.881957000	1.659430000	-3.261921000
H	1.965132000	1.837110000	-3.307865000
H	0.511674000	1.654132000	-4.297918000
H	0.735025000	0.646486000	-2.853371000
C	-1.542054000	3.012443000	2.394832000
H	-2.495371000	2.754439000	1.914999000
C	-1.436264000	2.178078000	3.678767000
H	-1.414972000	1.094697000	3.468145000
H	-2.312556000	2.363459000	4.316992000
H	-0.547993000	2.427847000	4.280014000
C	-1.582130000	4.520561000	2.720220000
H	-0.645705000	4.848635000	3.199701000
H	-2.411198000	4.739890000	3.410650000
H	-1.730878000	5.124133000	1.813465000
C	-0.690995000	2.821115000	-0.025797000
H	-2.966481000	-0.099306000	-0.053128000
H	2.930810000	0.130843000	-0.116486000

Appendix S2: The optimised cartesian coordinates of **8F**.

U	-0.023385000	0.002355000	-0.022790000
H	2.022666000	-5.459942000	-0.130789000
C	-0.607614000	-3.125344000	-2.071712000
Si	-3.374999000	-1.035251000	1.197915000
Si	-3.475427000	0.822180000	-1.190302000
Si	0.840690000	3.392376000	1.222182000
Si	2.432949000	2.525493000	-1.200275000
Si	2.547721000	-2.363321000	1.233419000
Si	1.080205000	-3.340338000	-1.221835000
H	0.822646000	-5.855703000	-1.386790000
H	0.286546000	-5.271997000	0.212094000
C	2.367158000	-3.341145000	-2.640667000

H	2.378856000	-2.352030000	-3.127961000
H	2.128831000	-4.099931000	-3.408869000
H	3.385244000	-3.542294000	-2.266753000
H	-1.443538000	-3.214612000	-1.357834000
H	4.870588000	-3.330977000	1.514579000
H	-0.743369000	-3.902415000	-2.845703000
H	-0.676687000	-2.136191000	-2.552722000
C	1.058022000	-5.151241000	-0.567695000
H	4.660746000	-2.683964000	-0.134108000
N	-2.602258000	-0.083557000	-0.014042000
N	1.238827000	2.237651000	0.008427000
N	1.376343000	-2.150285000	-0.013070000
F	-0.039590000	-0.072114000	2.246327000
F	0.005220000	0.064760000	-2.292836000
C	-2.274450000	-2.446942000	1.839145000
H	-1.998137000	-3.149837000	1.035490000
H	-2.805475000	-3.020857000	2.620246000
H	-1.346446000	-2.045470000	2.276221000
C	-4.982288000	-1.923749000	0.616469000
H	-5.773615000	-1.222438000	0.302560000
H	-5.392306000	-2.543681000	1.434964000
H	-4.772159000	-2.591499000	-0.236694000
C	-3.886497000	-0.032340000	2.743559000
H	-2.988847000	0.434537000	3.181208000
H	-4.354977000	-0.671500000	3.514648000
H	-4.596638000	0.772597000	2.488636000
C	-4.145884000	-0.242887000	-2.634456000
H	-4.844512000	-1.017375000	-2.275549000
H	-3.307055000	-0.754577000	-3.135472000
H	-4.673410000	0.370167000	-3.388474000
C	-2.428736000	2.184276000	-2.004512000
H	-1.536891000	1.750868000	-2.485502000
H	-2.087337000	2.935046000	-1.272021000
H	-3.023578000	2.711162000	-2.772528000
C	-5.012384000	1.749858000	-0.493150000
H	-5.770120000	1.066524000	-0.073958000
H	-5.501853000	2.344438000	-1.286512000
H	-4.712125000	2.444623000	0.310103000
C	-0.871250000	3.086121000	1.991032000
H	-1.677254000	3.142035000	1.240259000
H	-1.081705000	3.844427000	2.766837000
H	-0.911980000	2.089159000	2.458589000
C	0.769099000	5.212486000	0.598605000
H	1.737976000	5.568442000	0.209365000
H	0.470639000	5.890032000	1.419798000
H	0.026650000	5.317938000	-0.211038000
C	2.064332000	3.420555000	2.694306000
H	2.093982000	2.424711000	3.166650000

H	1.764614000	4.156791000	3.462952000
H	3.088418000	3.666528000	2.366486000
C	1.802319000	3.588832000	-2.662789000
H	0.931650000	3.093675000	-3.123510000
H	2.577545000	3.716144000	-3.440942000
H	1.483788000	4.591811000	-2.331632000
C	3.099056000	0.927405000	-1.984140000
H	3.537506000	0.249506000	-1.233468000
H	3.883532000	1.165344000	-2.725378000
H	2.286606000	0.384962000	-2.493523000
C	4.005491000	3.439173000	-0.564432000
H	3.785440000	4.441318000	-0.158799000
H	4.734630000	3.565627000	-1.385913000
H	4.497515000	2.858112000	0.234528000
C	3.155225000	-0.721887000	1.975765000
H	3.629091000	-0.075161000	1.219214000
H	3.900495000	-0.917712000	2.768077000
H	2.313850000	-0.166195000	2.419182000
C	1.908498000	-3.389739000	2.716657000
H	1.606998000	-4.405817000	2.410663000
H	1.024601000	-2.890020000	3.145847000
H	2.671880000	-3.483299000	3.511062000
C	4.161608000	-3.252005000	0.669760000
H	3.980676000	-4.272641000	0.292317000

Appendix S3: The optimised cartesian coordinates of **15F**.

U	5.109896000	2.701617000	-0.027479000
F	3.421247471	2.851154497	1.327144447
F	6.941537009	2.531310524	-1.178559761
P	4.312370000	6.329505000	-0.919504000
P	3.721797000	1.664621000	-3.430031000
P	4.915221000	-0.966624000	1.134955000
P	7.593460000	3.771038000	2.724342000
O	4.826552000	4.962307000	-0.611775000
O	3.948109000	2.074860000	-2.011286000
O	5.146730000	0.435878000	0.638374000
O	6.512028000	3.447580000	1.730975000
C	5.565952000	7.171283000	-1.933536000
C	5.916016000	6.603260000	-3.152993000
H	5.465804000	5.828146000	-3.400567000
C	6.896433000	7.096335000	-4.057356000
H	7.071439000	6.727515000	-4.892152000
C	7.540718000	8.161377000	-3.551977000
H	8.278962000	8.465112000	-4.028711000
C	7.255085000	8.778707000	-2.522804000
H	7.710273000	9.553821000	-2.285460000
C	6.155857000	8.236325000	-1.675731000

H	5.899109000	8.715594000	-0.920731000
C	4.030349000	7.246230000	0.591314000
C	4.535195000	6.780767000	1.800541000
H	5.026572000	5.991847000	1.823048000
C	4.308450000	7.482906000	2.964755000
H	4.680782000	7.169310000	3.756584000
C	3.577215000	8.595283000	2.997492000
H	3.332729000	9.001577000	3.797505000
C	3.198767000	9.119915000	1.747343000
H	2.788758000	9.954198000	1.722790000
C	3.399391000	8.471028000	0.583130000
H	3.116427000	8.845766000	-0.218929000
C	2.801436000	6.218662000	-1.872154000
C	2.576332000	7.023360000	-2.983169000
H	3.237075000	7.611106000	-3.271665000
C	1.373689000	6.954330000	-3.658372000
H	1.221610000	7.496712000	-4.399049000
C	0.377090000	6.049044000	-3.216421000
H	-0.426738000	5.976069000	-3.678833000
C	0.599021000	5.305487000	-2.140189000
H	-0.066681000	4.731548000	-1.837370000
C	1.825850000	5.370573000	-1.448617000
H	1.969911000	4.832135000	-0.703848000
C	4.028717000	3.017619000	-4.593426000
C	5.350820000	3.386439000	-4.816448000
H	6.045038000	2.954505000	-4.376543000
C	5.609899000	4.427813000	-5.720810000
H	6.488190000	4.684212000	-5.890634000
C	4.578233000	5.070783000	-6.355092000
H	4.750383000	5.774894000	-6.936176000
C	3.317423000	4.674351000	-6.130024000
H	2.618267000	5.122063000	-6.551514000
C	3.030929000	3.619170000	-5.289090000
H	2.156282000	3.321353000	-5.201109000
C	1.997661000	1.110405000	-3.639958000
C	1.063984000	1.666593000	-2.839944000
H	1.309957000	2.311536000	-2.217939000
C	-0.268687000	1.270161000	-2.950432000
H	-0.917246000	1.668566000	-2.414362000
C	-0.626464000	0.284011000	-3.854795000
H	-1.503776000	-0.021695000	-3.910039000
C	0.330347000	-0.214981000	-4.648670000
H	0.108430000	-0.857951000	-5.282951000
C	1.625838000	0.203147000	-4.540228000
H	2.265196000	-0.155812000	-5.111082000
C	4.805407000	0.280067000	-3.914131000
C	5.120368000	-0.644942000	-2.925879000
H	4.753539000	-0.562106000	-2.076761000

C	5.976032000	-1.690261000	-3.210283000
H	6.159904000	-2.315480000	-2.547356000
C	6.545278000	-1.826350000	-4.392911000
H	7.147413000	-2.520599000	-4.536136000
C	6.266579000	-1.001928000	-5.360702000
H	6.647529000	-1.143934000	-6.197544000
C	5.383348000	0.134116000	-5.172464000
H	5.211420000	0.735668000	-5.859943000
C	3.433776000	-1.680400000	0.413306000
C	2.445093000	-0.834283000	-0.049106000
H	2.544938000	0.086781000	0.034783000
C	1.306165000	-1.352998000	-0.632235000
H	0.643644000	-0.783003000	-0.951422000
C	1.156990000	-2.682328000	-0.738631000
H	0.391601000	-3.021564000	-1.143753000
C	2.096473000	-3.548168000	-0.270081000
H	1.960499000	-4.465287000	-0.345786000
C	3.257560000	-3.061010000	0.325325000
H	3.902053000	-3.644810000	0.656788000
C	6.341662000	-1.972300000	0.726355000
C	6.553966000	-3.232600000	1.235826000
H	5.911472000	-3.627060000	1.780080000
C	7.741090000	-3.930794000	0.935054000
H	7.876291000	-4.784800000	1.280839000
C	8.697864000	-3.356855000	0.132995000
H	9.477550000	-3.820345000	-0.069566000
C	8.493634000	-2.094583000	-0.368293000
H	9.148259000	-1.698150000	-0.896178000
C	7.339523000	-1.420056000	-0.098211000
H	7.209242000	-0.5777884000	-0.466504000
C	4.761313000	-1.019679000	2.913603000
C	4.127288000	-2.082749000	3.551977000
H	3.668966000	-2.731635000	3.069104000
C	4.202987000	-2.137973000	4.945350000
H	3.775001000	-2.838140000	5.383209000
C	4.874516000	-1.220854000	5.696257000
H	4.901866000	-1.291856000	6.623127000
C	5.504524000	-0.193285000	5.057884000
H	5.973962000	0.437851000	5.555079000
C	5.455959000	-0.078892000	3.666556000
H	5.887025000	0.629164000	3.243020000
C	8.432864000	2.283923000	3.255297000
C	8.547292000	1.242549000	2.355026000
H	8.159656000	1.307635000	1.512045000
C	9.241153000	0.096643000	2.717180000
H	9.301683000	-0.609441000	2.113590000
C	9.845563000	-0.019723000	3.948914000
H	10.272677000	-0.804698000	4.198535000

C	9.796335000	1.096599000	4.826678000
H	10.241113000	1.063070000	5.643060000
C	9.096501000	2.214893000	4.476800000
H	9.061999000	2.938727000	5.059930000
C	8.796881000	4.855803000	2.011286000
C	10.080479000	5.027393000	2.594416000
H	10.317004000	4.536290000	3.347370000
C	10.987149000	5.932678000	2.039931000
H	11.829773000	6.033266000	2.418454000
C	10.631459000	6.676235000	0.933008000
H	11.232675000	7.295538000	0.589268000
C	9.400009000	6.520424000	0.329417000
H	9.171464000	6.997720000	-0.435813000
C	8.515572000	5.615138000	0.912547000
H	7.674919000	5.520468000	0.525840000
C	6.909842000	4.650683000	4.139199000
C	7.565787000	5.672335000	4.777572000
H	8.422540000	5.918872000	4.511583000
C	6.946648000	6.327138000	5.814929000
H	7.378474000	7.047028000	6.215959000
C	5.727073000	5.962263000	6.269157000
H	5.342575000	6.409975000	6.989373000
C	5.064274000	4.932722000	5.669659000
H	4.218712000	4.690129000	5.966339000
C	5.653198000	4.244390000	4.615933000
H	5.217410000	3.520555000	4.227180000

References:

1. J. Wiebke, A. Moritz, X. Cao and M. Dolg, *Phys. Chem. Chem. Phys.*, 2007, **9**, 459-465.
2. P. D'Angelo, F. Martelli, R. Spezia, A. Filippini and M. A. Denecke, *Inorg. Chem.*, 2013, **52**, 10318-10324.
3. K. Leung and T. M. Nenoff, *J. Chem. Phys.*, 2012, **137**, 074502.
4. D. P. Halter, F. W. Heinemann, J. Bachmann and K. Meyer, *Nature*, 2016, **530**, 317-321.
5. M. J. Frisch, G. W. Trucks, H. B. Schlegel, G. E. Scuseria, M. A. Robb, J. R. Cheeseman, G. Scalmani, V. Barone, B. Mennucci, G. A. Petersson, H. Nakatsuji, M. Caricato, X. Li, H. P. Hratchian, A. F. Izmaylov, J. Bloino, G. Zheng, J. L. Sonnenberg, M. Hada, M. Ehara, K. Toyota, R. Fukuda, J. Hasegawa, M. Ishida, T. Nakajima, Y. Honda, O. Kitao, H. Nakai, T. Vreven, J. A. Montgomery, Jr., J. E. Peralta, F. Ogliaro, M. Bearpark, J. J. Heyd, E. Brothers, K. N. Kudin, V. N. Staroverov, R. Kobayashi, J. Normand, K. Raghavachari, A. Rendell, J. C. Burant, S. S. Iyengar, J. Tomasi, M. Cossi, N. Rega, J. M. Millam, M. Klene, J. E. Knox, J. B. Cross, V. Bakken, C. Adamo, J. Jaramillo, R. Gomperts, R. E. Stratmann, O. Yazyev, A. J. Austin, R. Cammi, C. Pomelli, J. W. Ochterski, R. L. Martin, K. Morokuma, V. G. Zakrzewski, G. A. Voth, P. Salvador, J. J. Dannenberg, S. Dapprich, A. D. Daniels, O. Farkas, J. B. Foresman, J. V. Ortiz, J. Ciosowski, and D. J. Fox, Gaussian, Inc., Wallingford CT, 2009.
6. A. D. Becke, *J. Chem. Phys.*, 1993, **98**, 5648-5652.
7. W. Ermler, R. Ross and P. Christiansen, *International journal of quantum chemistry*, 1991, **40**, 829-846.
8. G. Petersson and M. A. Al-Laham, *J. Chem. Phys.*, 1991, **94**, 6081-6090.
9. M. Llunell, D. Casanova, J. Cirera, P. Alemany and S. Alvarez, *Barcelona and Jersalem*, 2013.

10. F. Aquilante, J. Autschbach, R. K. Carlson, L. F. Chibotaru, M. G. Delcey, L. De Vico, I. Fdez. Galván, N. Ferré, L. M. Frutos and L. Gagliardi, *J. Comput. Chem.*, 2016, **37**, 506-541.
11. P. Å. Malmqvist, A. Rendell and B. O. Roos, *Journal of Physical Chemistry*, 1990, **94**, 5477-5482.
12. A. Wolf, M. Reiher and B. A. Hess, *J. Chem. Phys.*, 2002, **117**, 9215-9226.
13. L. F. Chibotaru and L. Ungur, *J. Chem. Phys.*, 2012, **137**, 064112.
14. F. Moro, D. P. Mills, S. T. Liddle and J. van Slageren, *Angew. Chem. Int. Ed.*, 2013, **125**, 3514-3517.
15. C. A. Goodwin, F. Tuna, E. J. McInnes, S. T. Liddle, J. McMaster, I. J. Vitorica-Yrezabal and D. P. Mills, *Chem. Eur. J.*, 2014, **20**, 14579-14583.
16. L. C. Pereira, C. m. Camp, J. T. Coutinho, L. Chatelain, P. Maldivi, M. Almeida and M. Mazzanti, *Inorg. Chem.*, 2014, **53**, 11809-11811.
17. A. Hervé, Y. Bouzidi, J.-C. Berthet, L. Belkhiri, P. Thuéry, A. Boucekkine and M. Ephritikhine, *Inorg. Chem.*, 2014, **53**, 6995-7013.
18. J.-C. Berthet, M. Nierlich and M. Ephritikhine, *Polyhedron*, 2003, **22**, 3475-3482.
19. J. D. Rinehart, K. R. Meihaus and J. R. Long, *J. Am. Chem. Soc.*, 2010, **132**, 7572-7573.
20. R. G. Surbella III and C. L. Cahill, *CrystEngComm*, 2014, **16**, 2352-2364.
21. J. T. Coutinho, M. A. Antunes, L. C. Pereira, J. Marçalo and M. Almeida, *ChemComm*, 2014, **50**, 10262-10264.
22. J.-C. Berthet, J.-M. Onno, F. Gupta, C. Rivière, P. Thuéry, M. Nierlich, C. Madic and M. Ephritikhine, *Polyhedron*, 2012, **45**, 107-125.
23. J.-C. Berthet, Y. Miquel, P. B. Iveson, M. Nierlich, P. Thuéry, C. Madic and M. Ephritikhine, *Journal of the Chemical Society, Dalton Transactions*, 2002, 3265-3272.
24. C. Apostolidis, B. Schimmelpfennig, N. Magnani, P. Lindqvist-Reis, O. Walter, R. Sykora, A. Morgenstern, E. Colineau, R. Caciuffo and R. Klenze, *Angew. Chem. Int. Ed.*, 2010, **122**, 6487-6491.
25. S. R. Daly and G. S. Girolami, *Inorg. Chem.*, 2010, **49**, 5157-5166.